

T-3712

DEPENDENCE OF COAL HYDROLIQUEFACTION

REACTIVITY ON COAL PROPERTIES

by

Sefa Yilmaz

ARTHUR LAKES LIBRARY
COLORADO SCHOOL of MINES
GOLDEN, COLORADO 80401

ProQuest Number: 10783477

All rights reserved

INFORMATION TO ALL USERS

The quality of this reproduction is dependent upon the quality of the copy submitted.

In the unlikely event that the author did not send a complete manuscript and there are missing pages, these will be noted. Also, if material had to be removed, a note will indicate the deletion.



ProQuest 10783477

Published by ProQuest LLC (2018). Copyright of the Dissertation is held by the Author.

All rights reserved.

This work is protected against unauthorized copying under Title 17, United States Code
Microform Edition © ProQuest LLC.


ProQuest LLC.
789 East Eisenhower Parkway
P.O. Box 1346
Ann Arbor, MI 48106 – 1346


T-3712

A thesis submitted to the Faculty and the Board of Trustees of the Colorado School of Mines in partial fulfillment of the requirements for the degree of Master of Science in Chemical and Petroleum-Refining Engineering.

Golden, Colorado

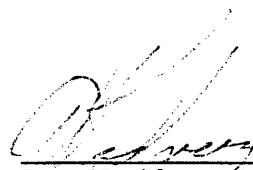
Date 6/26/1989

Signed: 
Sefa Yilmaz

Approved: 
Dr. Robert M. Baldwin
Thesis advisor

Golden, Colorado

Date 6/27/89


Dr. Arthur J. Kidnay
Department Head of Chemical
and Petroleum Refining
Engineering

ABSTRACT

The kinetics of hydroliquefaction for five coals from the Penn State Premium Coal Bank were studied in a tubing bomb micro-reactor system using a non-hydrogen donor vehicle. The goal of this study was to investigate the relationships between fundamental coal properties and coal hydroliquefaction reactivities. For experimental studies 1-methylnaphthlene was used as the non-hydrogen donor vehicle. Runs were made at three temperatures (425, 400, 375°C), five residence times (3, 5, 10, 15, 40 min), and 900 psi pressure. Five kinetic models were tested and a second order reversible model was determined to be the most adequate. Activation energies and rate constants for liquefaction of the five coals were also determined by using second order reversible model. Activation energies for conversion to THF solubles were correlated well with total carbon plus total hydrogen and activation energies for conversion to toluene solubles were highly correlated with free swelling index, total carbon, and total oxygen content. Rate constants were strongly correlated with total hydrogen content.

TABLE OF CONTENTS

	Page
ABSTRACT	iii
LIST OF FIGURES	vi
LIST OF TABLES	viii
ACKNOWLEDGEMENTS	ix
1. INTRODUCTION	1
2. LITERATURE SURVEY	3
2.1 Chemistry of Coal	3
2.2 Mechanism of Liquefaction	4
2.2.1 Methylene and Ether Bridges	6
2.2.2 Sulfur in Coal	10
2.2.3 Cross-Linking	11
2.3 Effect of Vehicles on Liquefaction	11
2.4 Kinetic Modelling	14
2.5 Correlation of Coal Reactivity	15
3. EXPERIMENTAL	21
3.1 Equipment	21
3.1.1 Tubing Bomb Reactor System	21
3.1.2 Analytical Equipment	23
3.2 Coals and Chemicals	25
3.2.1 Coals	25
3.2.2 Chemicals	26
3.3 Experimental Procedures	26
3.3.1 Run Procedure	26

3.3.2 Solvent Separation Analysis	30
4. EXPERIMENTAL DESIGN	33
4.1 Basic Argument	33
4.2 Detailed Experimental Matrix	34
5. RESULTS AND DISCUSSION	36
5.1 Definition of Conversion	36
5.2 Measurement of Kinetic Data	37
5.3 Kinetic Modelling	50
5.4 Correlations	61
5.4.1 Traditional Correlations	61
5.4.2 Correlation of Activation Energy	66
6. CONCLUSIONS	81
7. RECOMMENDATIONS	82
LITERATURE CITED	83
APPENDIX-1: Kinetic Data for 5 coals from Penn State Coal Bank	89
APPENDIX-2: Integrated Expressions for Kinetic Models ..	95
APPENDIX-3: Computer Program for the Calculation of SEE	96

LIST OF FIGURES

Figure	Page
1. The Macromolecular Network of Coal	4
2. Schematic Representation of the Reaction Cycles of Coal Hydrogenation	7
3. Schematic of Reaction System	22
4. Tubing Bomb Reactor	24
5. Schematic of Solvent Separation Procedure	31
6. Conversion to THF Solubles vs. Time Coal: Weir-Pittsburg	38
7. Conversion to THF Solubles vs. Time Coal: Bevier-Wheeler	39
8. Conversion to THF Solubles vs. Time Coal: Lower Freeport	40
9. Conversion to THF Solubles vs. Time Coal: Lower Sudduth	41
10. Conversion to THF Solubles vs. Time Coal: Splashdam	42
11. Conversion to Toluene Solubles vs. Time Coal: Wier-Pittsburg	43
12. Conversion to Toluene Solubles vs. Time Coal: Bevier-Wheeler	44
13. Conversion to Toluene Solubles vs. Time Coal: Lower Freeport	45
14. Conversion to Toluene Solubles vs Time Coal: Lower Sudduth	46
15. Conversion to Toluene Solubles vs. Time Coal: Splashdam	47
16. Arrhenius Plot (THF Solubles) Model: Second Reversible	59

17. Arrhenius Plot (Toluene Solubles) Model: Second Reversible	60
18. Conversion to Toluene Solubles vs. (C+O) Content (5 min,425°C)	63
19. Conversion to Toluene Solubles vs. (C+O) Content (5 min,400°C)	64
20. Conversion to Toluene Solubles vs. (C+O) Content (5 min,375°C)	65
21. Correlation of Kinetic Constant (Toluene Sol.) vs. Total Hydrogen. Temperature: 425°C	67
22. Correlation of Kinetic Constant (Toluene Sol.) vs. Total Hydrogen. Temperature: 400°C	68
23. Correlation of Kinetic Constant (Toluene Sol.) vs. Total Hydrogen. Temperature: 375°C	69
24. Correlation of Activation Energy (THF Sol.) vs. C+H	72
25. Correlation of Activation Energy (Toluene Sol.) vs. Index+(C*O)	73
26. Correlation of Activation Energy (Toluene Sol.) vs. Index+(H*O)	74
27. Correlation of Observed and Calculated Rate Constant (THF Solubles)	77
28. Correlation of Observed and Calculated Rate Constant (Toluene Solubles)	78

LIST OF TABLES

Table	Page
1. Characterization Data of Penn State Coal Sample Bank (Ultimate Analysis)	27
2. Characterization Data of Penn State Coal Sample Bank (Proximate Analysis)	28
3. Free Swelling Index of Coals	49
4. Kinetic Models	51
5. Statistical Comparison of Kinetic Models (THF Solubles)	52
6. Statistical Comparison of Kinetic Models (Toluene Solubles)	53
7. Algorithm of the Calculation SEE	54
8. Activation Energy (THF Sol.) and Kinetic Constants. Model: Second Reversible	56
9. Activation Energy (Toluene Sol.) and Kinetic Constants. Model: Second Reversible	57
10. Coal Ranking with Respect to Activation Energy (Toluene Solubles)	58
11. R-Square Values of Point-Yield Conversion (Toluene Solubles) vs. total C+O Content	62
12. Stepwise Regression of Coal Properties in Predicting Activation Energy (THF)	70
13. Correlations of Activation Energy, Frequency Factor with Coal Properties	79

ACKNOWLEDGEMENTS

I wish to express my sincere gratitude to Dr. Robert Baldwin for his guidance and advice throughout the course of my graduate studies. I also would like to express my thanks to Dr. Ronald Miller and Dr. Sung-Chul Shin for helpful communications and friendship.

I am also very grateful for the financial that I have received from the Turkish Petroleum Refineries Inc. (TUPRAS).

Finally, thanks is not enough for the love and support received from my wife, Semra, without her encouragement, I may never have finished. Thank you.

1. INTRODUCTION

The goal of developing a fundamental understanding of the chemistry of coal has been occupying researchers for over half a century. Techniques available for analysis of coal are not as yet powerful enough to give a detailed description of coal unit structures, since coal is an inhomogeneous mixture of organic and inorganic species. Today much research is focused on reactions typical of coal, but using homogeneous substances with known structures (model compounds) as well as instrumental techniques that give direct information about the structure of coal.

The main purpose of much of the research on coal is to produce an energy source for future usage as a substitute for petroleum. To achieve this goal one has to fully understand the characteristics and behavior of coal under certain conversion conditions. However, the research on coal conversion that has been done generally lacks fundamental definitions for reactivity. Coal hydroliquefaction reactivity is usually defined as the conversion rate to some solvent soluble classification at fixed temperature and time. It has been proven that this type of definition may give rise to incorrect conclusions about the characteristic behavior of coal for conditions other than those for which they were produced. Recently, new reports have been published expanding the question of how to define and correlate

coal liquefaction reactivity based on rate processes. Furlong showed that the rate of reaction served as a more sensitive relative reactivity ranking parameter than the conversion for coals with very similar composition (40). However, this definition was shown to be flawed by Shin (23), who pointed out that two coals with the same kinetic constants may also show different conversions at long reaction times.

In this study, activation energy is used as a more general reactivity parameter for coal hydroliquefaction. Correlation of coal properties with activation energies for conversion to THF and toluene solubles is carried out, and relationships to coal structure and the chemistry of coal liquefaction developed. Finally, reactivity ranking using activation energy as the parameter is shown to be independent of the choice of kinetic model.

2. LITERATURE SURVEY

Production of liquid fuels from coal has been a technical feasibility since the late 19th century. The possibility of producing a liquid-like material from coal was first demonstrated by Bertholet in 1869. Germany laid the foundations for most of the present day direct and indirect coal liquefaction techniques with the discovery and development of the Bergius hydrogen donor process in 1913, the Pott-Broche solvent extraction process in 1927, and the Fischer-Tropsch process for hydrocarbon synthesis from synthesis gas in 1925 (1).

2.1 Chemistry of Coal

The goal of developing a fundamental understanding of the chemistry and structure of coal has been occupying researchers for over half a century. Coal is a sedimentary rock which accumulated initially as peat. Virgin coal is composed principally of macerals (plant fossils) and subordinately of minerals, water, and gases in submicroscopic pores. Coal is an inhomogeneous mixture of carbon, hydrogen, oxygen, sulphur, and minor proportions of other elements (2). As shown in Figure 1, coal is considered to contain relatively small polycyclic aromatic and hydroaromatic rings as structural units, connected by ether and

methylene bridges to form a macromolecular structure (3). Thus conversion of coal via depolymerization is believed to proceed initially mainly through cleavage of these bridges.

2.2 Mechanism of Liquefaction

The reactivity of coal in liquefaction reactions is influenced by its chemical structure. Hence, a knowledge of the relationship between reactivity and chemical structure is useful for the elucidation of the liquefaction mechanism.

To produce liquids from coal, the following chemical changes need to be accomplished :

- Breaking large macromolecular structures into smaller ones by bond rupture.

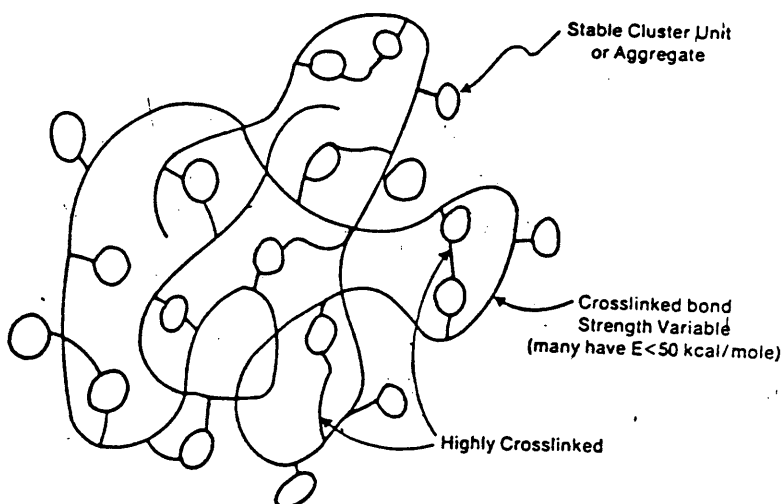


Figure 1. The macromolecular network of coal (3)

- Addition of hydrogen to increase H/C atomic ratio.
- Removal of heteroatomic species (N, O, S) by transformation into their hydrogenated gas state (H₂O, H₂S, etc.).
- Removal of mineral matter.

Presently, there are no standard methods or techniques to separate and characterize liquids from coal. However, most investigators in coal liquefaction tend to characterize coal-derived products by solubility distribution analysis, chromatographic analysis, and distillation (4, 5, 6). Among these three techniques, solubility distribution (solvent extraction) is most commonly used by researchers to characterize coal products and to define coal conversion. The solvent extraction technique classifies coal-derived products into lumped groups of compounds according to their relative solubilities in different solvents such as tetrahydrofuran (THF), toluene, hexane, etc. Lumped groups which are most widely named are "preasphaltenes" (soluble in polar solvents such as THF or pyridine, but insoluble in non-polar aromatic solvents such as benzene), "asphaltenes" (soluble in benzene but insoluble in hexane), and "oils" (soluble in hexane). The molecular weight of the molecules in the above fractions are correspondingly smaller than the molecular weight of the parent coal; the lower molecular weight results from various bond-breaking reactions.

Pyrolysis of coal is presumed to be the first step in which the structure of coal is broken down to smaller fragments by thermal bond rupture. The resulting derived fragments (radicals) are assumed to capture hydrogen from hydrogen donor species such as tetralin, dihydrophenanthrene (DHP), from molecular hydrogen supplied either directly or indirectly by the gaseous reaction atmosphere, or from hydrogen-rich portion of the coal itself. A schematic representation of hydrogenation of coal in the presence of a hydrotreating catalyst and a donor solvent is shown in Figure 2.

The mechanism of direct hydroliquefaction is widely believed to proceed by a free-radical mechanism (7). Thermal cleavage of C-C, C-O and C-H bonds are assumed to initiate the free-radical processes, and it has been shown by Benjamin (8) that C-C cleavage can occur under the conditions of asphaltene formation.

2.2.1 Methylene and Ether Bridges

It has been generally accepted that there are ether and methylene bridges in coal, and that breaking these bonds initiates thermal conversion and thus the liquefaction of coal. To understand the contribution of these bridges to the mechanism of liquefaction, reactions using various model

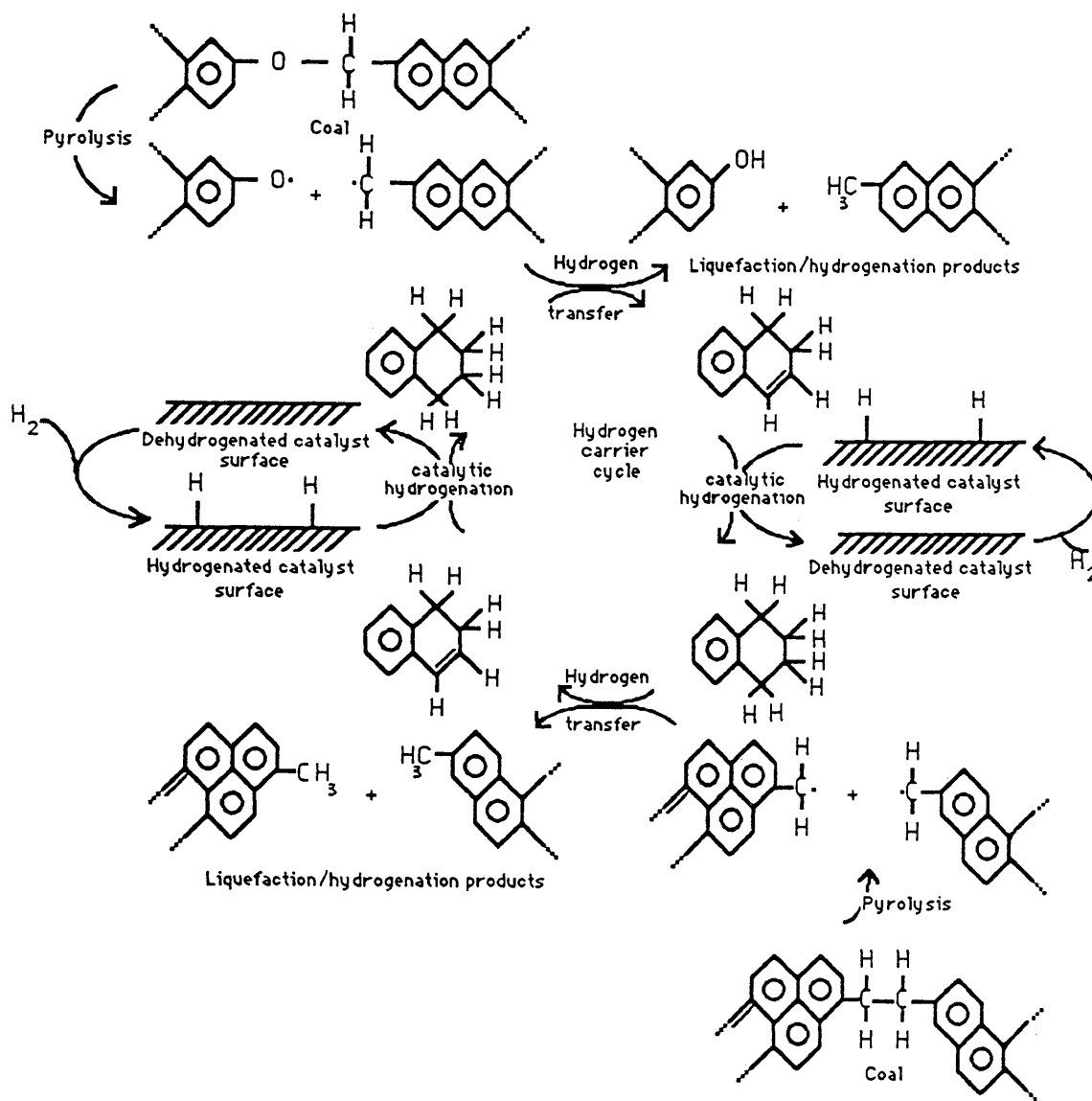


Figure 2. Schematic Representation of the Reaction Cycles of Coal Hydrogenation (69)

compounds have been studied. As the simplest model for methylene connecting units in coal, thermolysis of $\text{Ar-CH}_2\text{-X-Ar'}$ ($\text{X}=\text{CH}_2, \text{O}, \text{S}$) model compounds has been of particular interest. Poutsma (9) studied the thermolysis of both gaseous and liquid dibenzyl and concluded that the results for thermolysis of dibenzyl are consistent with a nonchain, free radical mechanism but only after appropriate account is taken for combination, disproportionation (another disappearance pathway for radicals), and rearrangement of the radicals involved. The effect of the number of methylene groups and substituents in etheric structures on the mechanism of thermolysis has been studied by many researchers (10, 11, 12, 13, 14, 15). Korobkov (10) showed that introducing methylene groups into a Ph-O-Ph structure drastically decreased its stability. He further found that introducing additional methylene groups into R-O-R structure had a two fold effect: In the nonsymmetrical structures such as $\text{Ph-CH}_2\text{CH}_2\text{-O-Ph}$, C-O bond strength remained low; in symmetrical structures, like $\text{Ph-CH}_2\text{-O-CH}_2\text{-Ph}$ or $\text{Ph-CH}_2\text{CH}_2\text{-O-CH}_2\text{CH}_2\text{-Ph}$ bond strength increased. Yoshida (16) found that the cleavage of ether bridges contributed to the formation of preasphaltenes. He also found that the conversion to hexane solubles in the mild liquefaction reaction (400°C , 30 min) correlated well with CH_2 carbon content of coal. Yoshida further concluded that the formation of oil from

preasphaltenes was caused by scission of CH₂ bridges and some naphthenic CH₂ bonds. He also determined that etheric oxygens in coal are distributed predominately as aromatic rather than aliphatic ethers. From an extensive model compound study, Benjamin (8) showed that structures that contain two-carbon aliphatic chains as bridges connecting aryl groups are cleaved from the central C-C bonds, not the bonds adjacent to the aryl rings. Benjamin further showed that preasphaltenes were formed in part by the scission of C-C bonds in ethylene bridges connecting aryl groups, and that the slower asphaltene and oil formation must be partly a result of ether bond cleavage and more C-C bond cleavage including bonds adjacent to aryl rings. Kamiya (17) proved that the conversion rate of 2, 2' dinaphthyl ether was remarkably enhanced in the presence of hydrogen donor solvent. It was postulated by Kamiya that the enhancing effect of the hydrogen donor was due to hydrogen transfer to the aromatic nucleus of the diaryl ether from the hydrogen donor, and successively fast decomposition of the hydrogenated ether. From the study of pyrolysis of dibenzyl ether at 450°C, Schlosberg (18) found that in the absence of added hydrogen, increasing reaction severity (residence time) led to growth/polymerization reactions ultimately leading to coke.

2.2.2 Sulfur in Coal

Compounds of nitrogen and sulfur are also components of coal, and their removal is of economic importance in producing clean fuels from coal. Sulfur in coal exists as both inorganic (pyrite, FeS_2 , etc.) and organic sulfur (thiophene etc.) compounds. The effect of pyrite (FeS_2) on coal liquefaction reactivity has been studied by many researchers. Guin (65) studied both the effect of elemental iron and iron sulfide (FeS_2) as a catalyst on the liquefaction reactivity of coal and rate of hydrosulfurization. He reported that elemental iron had very little catalytic activity towards the liquefaction reactivity of coal, but it acted as a very strong sulfur scavenger by reacting with hydrogen sulfide (H_2S) to produce a nonstoichiometric iron sulfide $\text{FeS}(1+X)$. Guin (65) further showed that iron sulfides catalyzed the coal liquefaction reaction resulting in higher oil yields, but they did not affect the removal of sulfur from the coal liquids. Mukherjee (68) also studied the effect of mineral content on liquefaction reactivity and reported that conversion to liquid products increased with increasing mineral matter, with iron pyrite identified as an active catalyst. Baldwin (66) suggested that pyrite may be acting as an indirect catalytic agent via formation of H_2S . It has been shown that most of the sulfur removal by catalytic hydrogenation was from a R-S-R type structure

rather than thiophene like structures (67).

2.2.3 Cross-linking

It is known that when coal is immersed in a solvent the solvent penetrates into and causes swelling of the coal.

The degree of cross-linking can be estimated by the swelling behaviour of the coal. Larsen (20) estimated the degree of cross-linking (average molecular weight per cross-link) by using data based on solvent swelling (amine bases) and the interaction of the swelling molecules with coal. In those swelling experiments, Larsen (21) further showed that low rank coals, like lignite and subbituminous, have a much higher tolerance to branched, bulky groups than do the bituminous coals. Ouchi (22) stated that higher conversions of lower rank coals probably results from the fact that these coals contain more ether linkages which are easily cleaved, and more polar functional groups such as hydroxyl or carboxyl groups which contribute to the enhancement of cleavage of C-C linkages.

2.3 Effect of Vehicle (Solvent) on Liquefaction

Much research has been carried out to determine the effects of various vehicles (non-hydrogen donor and hydrogen donor) on coal hydroliquefaction and the function of gaseous hydrogen as a hydrogen donor source. Shin (23) performed

experiments with 5 bituminous coals in 1-methylnaphthalene (1-MN), naphthalene, and phenanthrene (non H-donor vehicles), and the relative reactivities of these coals was assessed by toluene conversion. His data clearly showed that the relative reactivities were independent of the choice of non-H donor vehicle.

It was proposed by Ouchi that when the reactivity of the coal was higher than that of the solvent, the coal appeared to be predominantly hydrogenated directly by gaseous hydrogen (22). When reactivity of the coal approaches that of the solvent, an alternative mechanism begins to operate in which the solvent is hydrogenated initially to form a donor solvent which then donates hydrogen to the coal. If the solvent reactivity is greater than that of coal, the second path predominates. In 1976, Neavel (24) showed that free radicals formed pyrolytically were stabilized in the early stages by autogenous hydrogen transfer, and in later stages by abstraction of hydrogen from the hydrogen-donating tetralin. Utz (25) studied short contact time liquefaction in hydrogen-donor and gaseous hydrogen vehicles and found that even though hydrogen consumption is minimal during the early stages of liquefaction, hydrogen-donor vehicle plays an important role in converting coal to THF-soluble materials. Utz further found that H₂ was a competing source of hydrogen in short contact time liquefac-

tion, and that the rate of reaction of H₂ with reactive coal fragments (free-radicals) was similar to that of tetralin. Winschel (26) showed that donor solvent quality (as measured by microautoclave coal conversion) increases with increasing hydroaromatic content and with decreasing aromaticity and paraffinicity.

Effect of Phenolic Compounds on Liquefaction

Among organic substances, phenols have a particularly individual set of chemical properties. ✓ Earlier work (27) had shown that a major fraction of the oxygen in vitrinites and vitrains was present as phenolic OH. ✓ As early as 1955, Brown (28) showed that a decrease in the intensity of the phenolic OH band was one of the first phenomena to be observed when vitrinites were pyrolysed at temperatures of 400-550°C. From these findings, Abdel-Baset suggested that dissociation of OH to produce free radicals might deepen hydrogenation of coal structures (29). It was confirmed that phenolic compounds are not effective solvents for coal dissolution in the absence of a hydrogen donor (30). Phenols do have a remarkably positive effect on coal liquefaction in the presence of tetralin, depending on the character of the coal and on the concentration of the phenols. Kamiya (30) found that the solvent refined coal obtained in the presence of phenol was low in hydrogen content and high in aromatic

hydrogen. These results are in agreement with the fact that coal conversion increases without the simultaneous increase of hydrogen consumption in the presence of phenols.

2.4 Kinetic Modelling

Initially work on kinetic modelling of coal liquefaction was done in the 1940's by Storch who defined the products of liquefaction by lumped groups in terms of solubility of the products in acetone and benzene (31). Curran (50) defined the kinetics of coal conversion by assuming that a certain portion of the coal dissociated at a faster rate than the remaining part. In 1968, Wiser (51) reported that second order reactions in the initial stages of liquefaction shifted gradually to first order reactions at longer reaction time. Many kinetic models have been proposed to involve entire reaction networks by assuming pseudo-first order reactions for each reaction step (35, 52). Following the assumption of various reaction paths among lumped coal-derived products, best-fit models were obtained for the experimental data by using regression schemes. In spite of the fact that the experimental data can be described satisfactorily, it is generally understood that these kinetic models do not necessarily represent the true reaction mechanism because more than one rate constant can be obtained from statistical analysis (42, 43, 44). Recently

Anthony (45, 46) proposed statistical kinetic models based on the concept of a distribution of activation energies. More recently Shin (53) developed a single-step liquefaction kinetic model by using a pseudo-equilibrium conversion concept.

2.5 Correlation of Coal Reactivity

Many researchers have attempted to find satisfactory correlations between properties of parent coal and coal liquefaction behavior. Bergius (54) in 1920 recognized that coals with over 85% carbon (d.a.f. basis) made poor liquefaction feedstocks; but it was later found that coal rank was not adequate in assessing the liquefaction behavior of a coal (55). In Germany, the Institute of Technical Chemistry compared the relative ease of coal liquefaction to a benzene-soluble product (no catalyst or organic carrier solvent was used) and their results indicated that in the range from 52% to 84% carbon content by weight (moisture free), conversion tends to increase with increasing H/C or O/C ratios of feed (32). Fischer and his co-workers (56) in 1942 carried out an extensive research program to determine the relationship between petrographic composition of coal with coal liquefaction reactivity, but their study was a limited success. It was later found that coals of the same overall carbon content may have different maceral distributions

(57). In 1951, one of the earliest models for the liquefaction of bituminous Dutch coals using anthracene oil and beta-naphtol as solvents was proposed by Oele et al (33). The rate data obtained by these researchers were correlated with a reversible model, assuming that forward reaction was zero order and that reverse reaction was first order with respect to the fraction of extracted material.

Hill et al. (34) proposed the following kinetic expression for the liquefaction of high-volatile bituminous coal in tetralin:

$$dX/dt = k(1-X)$$

where "X" is the fraction of coal liquefied and "k" is the first order rate constant which was modeled as a function of conversion:

$$k = k_0(1-aX)$$

Here, "k₀" is a pseudo second-order rate constant and "a" is the reciprocal of the maximum liquefiable fraction at a given temperature.

It is often observed that the fraction of bituminous coal liquefied in tetralin, determined by soxhlet extraction using benzene, increases with increasing temperature and finally reaches an "equilibrium" value beyond which

it remains constant. The time required to reach this "equilibrium" value is seen to decrease with increasing temperature, while the "equilibrium" value attained increases with increasing temperature. Cronauer et al. (35) observed an increase in this "equilibrium" value for a given coal with increasing hydrogen-donor capacity of the solvent used to liquefy the coal.

In the second half of 1970's Given et al. completed extensive liquefaction reactivity research with more than one hundred different coals. Correlation studies on these coals provided insight into the nature of coal reactivity (36,37,38,39). The results of their work can be summarized as follows:

- Attempts to correlate coal properties solely with a rank parameter, such as carbon content, are not adequate.
- Geographic origin is one of the key factors affecting coal liquefaction behavior.
- The liquefaction behavior of coals can vary widely depending on their chemical and petrographic characteristics.
- Sulfur content is one of the major factors in defining coal reactivity populations.

As a measure of coal reactivity, Given used the percentage of coal converted to ethyl acetate soluble products for a reaction time of 60 minutes.

The concept of point-yield conversion at a given residence time as the definition of reactivity has been used by many researchers. However this definition of reactivity does not provide any insight into the kinetic behavior of the coal. Previously, only a few reports have been published correlating kinetic parameters with coal properties. Correlation of basic coal properties with kinetic parameters was initiated by Furlong (58) and Gutmann (63). Furlong (40) later proposed that a kinetically defined reactivity would have a more direct correlation with parent coal properties rather than a reactivity defined by a single point conversion. Furlong further showed that a kinetic definition for reactivity was superior in ranking relative reactivities among closely related coals (58). More recently Shin (53) proposed a different concept which combined both static and dynamic reactivity definitions as a measure of the liquefaction reactivity of coal. He developed this idea further and correlated liquefaction activation energies for toluene solubles with coal properties, choosing a first-second order reversible model as the best kinetic model from five proposed models (23).

Most of the research done earlier was intended to separate coal liquids into "kinetically similar lumped groups" such as by solubility in various solvents or using liquid-solid chromatography (LSC) or distillation. Many

researchers have attempted to quantitatively relate coal liquefaction yields to basic coal properties (e.g., volatile matter, H/C atomic ratio, reactive macerals, fixed carbon, sulfur content, etc.). Neavel (47) studied interrelationships between coal compositional parameters and reported that many derived properties (density, reflectance, specific energy, free index, and volatile matter) of coal have a strong interrelationship with the elemental properties of the coal. Neill (59, 60) also determined that a high correlation existed between aromaticity and the carbon content of coal. Neavel (61) pointed out the necessity of correlation with basic properties of the coal, and not with derived properties. Although correlation between coal fundamental properties and liquefaction yield has been thoroughly studied, only a few correlational studies have been made concerning the kinetic behavior of coal in direct hydroliquefaction. Prasad (62) collected the reported values for activation energies from other researchers and concluded that there appeared to be a direct correlation between activation energy and elemental (H/C) ratio of the coal. Gutman (63) calculated the kinetic rate constants for 10 lignite coals by assuming a series first-order model, and found that kinetic constants had some correlation with combustible sulfur contents of the coals. Shin (23) recently found a strong correlation between activation energy (THF

solubles) and aliphatic hydrogen content. He also reported satisfactory correlations between activation energy (toluene solubles), total oxygen (wt%) and protonated aliphatic carbon (wt%). Most recently Neill (48) found that, from a set of 26 high volatile bituminous coals with sulfur contents ranging from 2.8 to 7.9% by weight, there was a tendency for total conversion to decrease with increasing rank. In addition no correlation of asphaltenes, oils, gas, rank or sulfur content were seen. Shadle (49) recently found that no correlation existed between liquefaction yields from 26 high-sulfur coals and structural features, and stated that high sulfur coals were more heterogenous than had been expected.

3. EXPERIMENTAL

3.1 Equipment

3.1.1. Tubing-Bomb Reactor System

An existing tubing bomb reaction apparatus was used to carry out the experimental portion of this research. A schematic of this apparatus is shown in Figure 3. This unit, used for coal liquefaction reactions, was previously employed by Altizer and is described in detail in his thesis (50). The system consists of four subsystems: gas feed subsystem, gas sampling subsystem, heating, and reactor subsystems.

The gas feed subsystem is designed to permit precise control of feed gas pressure to the reactor. The reactor subsystem is evacuated first through valve V5 with valve V3 closed, insuring the integrity of the gas mixture fed to the reactor. The gas sampling subsystem consists of a one liter surge tank with a Swagelok female quick connect sample port, allowing sampling of the reaction product gases. Valve V5, a Whitey micro-metering valve, allows for the reactor tube to be pressurized accurately. The heating system, designed to rapidly attain the desired reaction temperature, utilizes a Tecam Model SBL2D fluidized bed sand bath. The bath temperature is controlled by a Leeds & Northrup Electromax III temperature controller connected to a Leeds & Northrup model

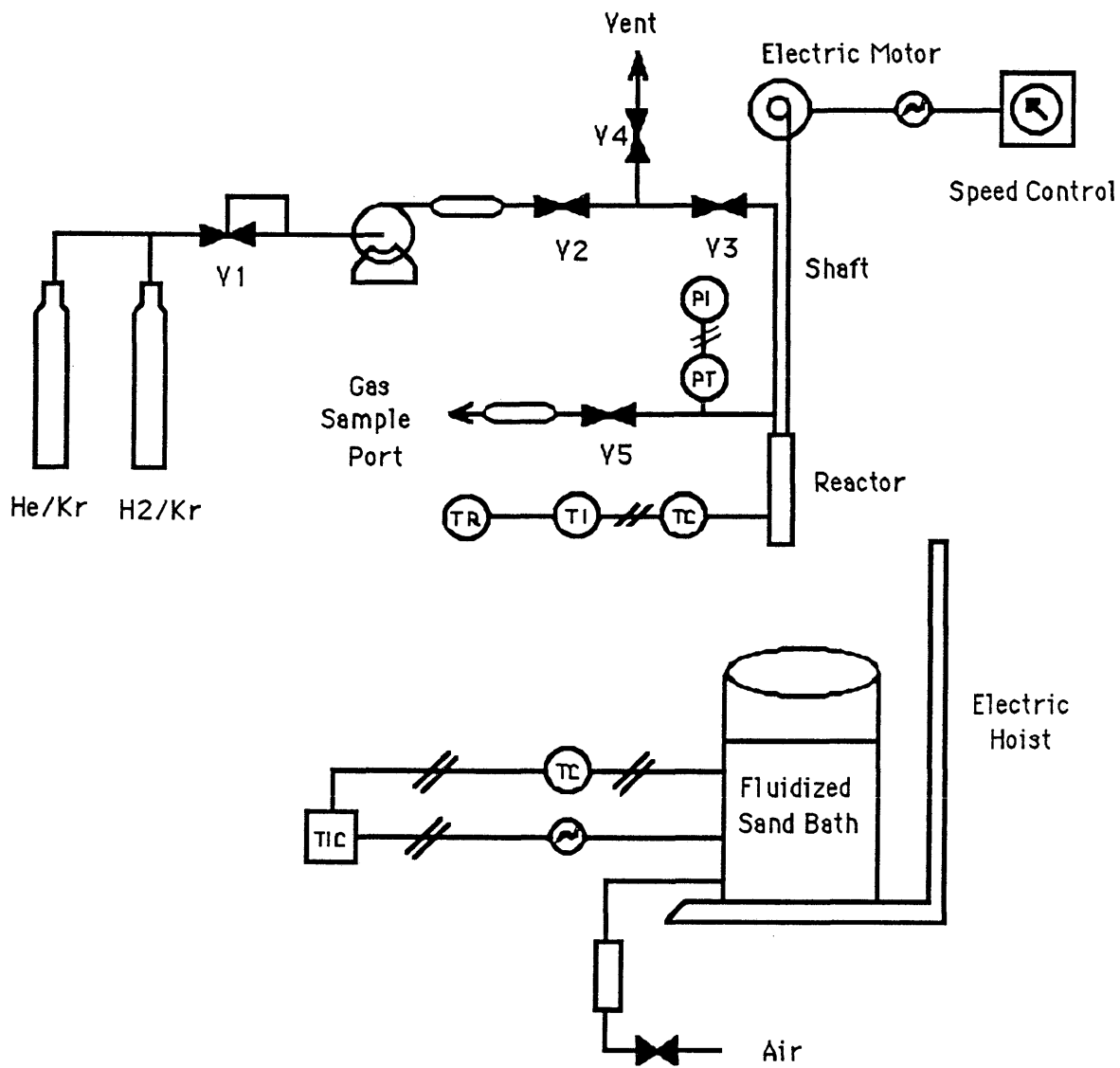


Figure 3. Schematic of Reaction System

1106 zero voltage power supply. The reactor contents were found to attain the desired temperature within 3 minutes after immersion into fluidized bed sand bath.

A drawing of the tubing-bomb reactor assembly is shown in Figure 4. The body of the reactor consists of 1/2" OD 316 stainless steel tubing, closed at the bottom by a swagelok 1/2" cap and welded at the top to a Cajon VCR gland-type gasket fitting. The reactor head is a combination of a VCR gland fitting, a Swagelok male run tee, a K type thermocouple in a 1/16" stainless steel sheath, and a 1/8" Autoclave Engineers union on the gas feed line. Reactor volume is approximately 20 cc for the tubing-bomb. Ten reactors of the described configuration were fabricated for experimental use. A disposable nickel gasket was used for sealing purposes. This "zero-clearance" type of fitting has been found to be far superior to other closure systems employed in this laboratory (Swagelok compression fitting) in terms of re-use and ease of pressure seal. The reactor is agitated vertically by use of an eccentric arm driven at a rate of approximately 120 rpm.

3.1.2 Analytical Equipment

Analytical procedures used in this research were identical to those employed by Shin (23). The solvent separation analysis requires that the samples be dispersed using a

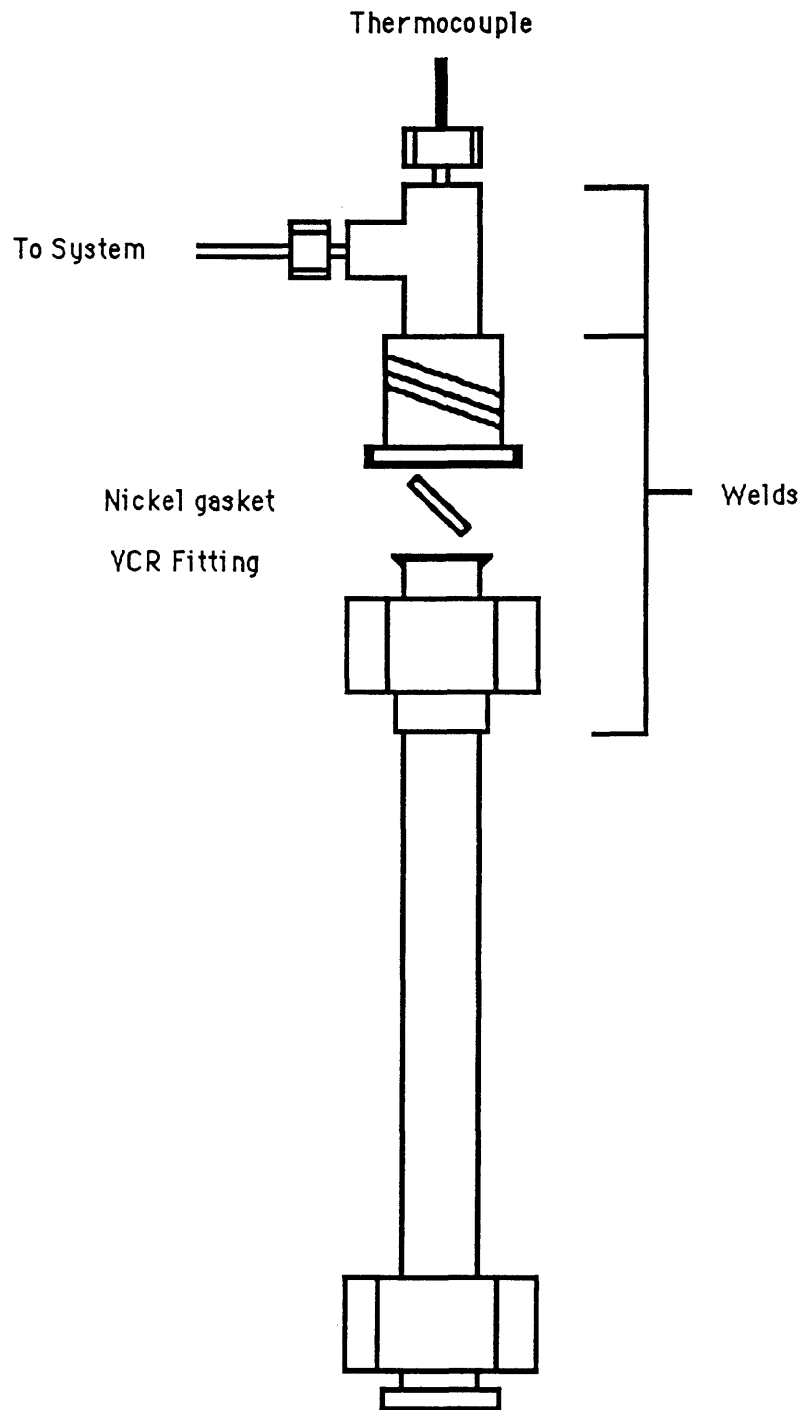


Figure 4. Tubing-bomb Reactor

sonic bath, centrifuged, and dried. To perform these steps, a Branisonic Ultrasonic bath, an IFC Dacmon Model ICX centrifuge, and a Precision Scientific Oven were used. Two rotary evaporators manufactured by Buchi were used for solvent recovery of THF from the soluble liquefaction products. A Mettler PC 2000 top-loading electronic balance with a precision of 0.01 gram was used for reactor charge and liquid product weights.

A model 111H Carle analytical gas chromatograph was used in conjunction with a model 3390A Hewlet-Packard integrator for gas analysis.

3.2 Coals and Chemicals

3.2.1 Coals

Five different bituminous coals ranging from high volatile to low volatile were used in this study. Fifteen coal samples were purchased from the Penn State Premium Coal Sample Bank. Every effort was made by Penn State Premium Coal Bank to obtain coal samples from the most recently exposed areas of a coal mine and samples were stored in containers under an inert gas. Nine of the samples purchased (ground to -60 mesh or 250 micron) arrived in ampules and six samples (ground to -20 mesh) were shipped in cans. Prior to experimentation, all samples were ground to -100 mesh (150 micron). This was performed in a Labconco glove

box under a nitrogen blanket in order to avoid oxidation. The ground samples were then sealed in small amber borosilicate glasses and stored in a Labconco Vacuum dessicator. From fifteen coal samples, five were chosen and used for the experiments. Preliminary characterization data for these coals are given in Tables 1 and 2.

3.2.2 Chemicals

The chemicals utilized in this research were obtained from Aldrich Chemical Company and were used as received without further purification. A gaseous mixture of 99 mole % hydrogen and 1 mole % krypton tracer was used as feed gas (Liquid Air Corporation).

3.3 Experimental Procedures

3.3.1 Run Procedure

Start-Up

1. Air is introduced to the sand bath to induce fluidization. Bath temperature is set to the desired reaction temperature and monitored with a type K thermocouple.

2. Air flowrate is adjusted during heat up to prevent excessive bubbling of the sand bath.

3. Approximately 3 hours is required for the sand bath to reach the proper operating temperature.

Run Preparation

1. The reactor is charged with 1.0 gram of coal, 1.0

Table 1. Characterization Data of Penn State Coal Sample Bank (Ultimate Analysis)

Coal Seam	State	Rank	Ultimate Analysis				Ash
			C	H	O	Stot	
Weir-Pittsburg	MO	HVAB	78.4	5.7	1.7	12.5	17.9
Bevier-Wheeler	MO	HVBB	78.0	5.7	6.7	8.0	20.5
Lower Sudduth	CO	HVCB	68.2	5.3	24.5	0.7	31.3
Splashdam	VA	MVB	87.5	5.4	4.8	0.8	12.4
Lower Freeport	PA	LVB	89.1	4.6	3.8	1.7	21.6

Note:

1. All the values are on a moisture and ash-free basis (wt%), except for "ash", which is in dry wt%.

2. Data furnished by Penn State Coal Bank.

Table 2. Characterization Data of Penn State Coal Sample Bank (Proximate Analysis)

Coal Seam	State	Rank	Moisture	Ash	V.M	F.C
-----	-----	-----	-----	-----	-----	-----
Weir-Pittsburg	MO	HVAB	6.3	16.8	37.2	39.8
Bevier-Wheeler	MO	HVBB	9.3	18.6	34.8	37.4
Lower Sudduth	CO	HVCB	5.8	29.5	32.7	32.0
Splashdam	VA	MVB	1.6	12.2	27.0	59.2
Lower Freeport	PA	LVB	0.5	21,5	16.6	61.4

Note:

1. All the values are based on "as received" basis (wt%).
2. Data are furnished by Penn State Coal Bank.

gram of the vehicle, and two small stainless mixing balls.

2. The reactor is then sealed into the VCR fitting using the nickel gasket.

3. The reactor system is then attached to the eccentric arm. Following this, the reactor and gas surge tank are evacuated. Valve V3 is closed during evacuation. After the reactor is evacuated, valve V5 is closed, preventing backflow of air into the reactor.

4. Reactor is then charged with the reaction gas to the desired pressure by opening the metering valve V2 smoothly. Then V2 and V3 are closed.

5. Following pressurization, the system is monitored for gas leaks by observing the system pressure.

Reaction Procedure

1. First eccentric arm is activated.

2. Reaction is started by raising the fluidized bed to the indicated level immersing the reactor. Time zero is defined as when the reactor is first immersed in the sand bath.

3. The sand bath is lowered after the allotted reaction time, and reaction is then terminated by first quenching the reactor with cold air, and then quenching the reactor in ice water.

4. Gas is then bled to the gas sampling bottle by opening V5 slowly. The sample bottle consists of an evacu-

ated 75 ml stainless steel pressure vessel.

Unit Shut Down

1. Turn off the panel controls and shut off the gas cylinder.

2. Vent the remaining gas in the system to blowdown.

3.3.2 Solvent Separation Analysis

The liquid products from the reactor were collected into a 250 ml centrifuge tube by washing the reactor with THF. Product recovery from the reactor was 100 %. Following this, the reaction slurry was analyzed via the solvent separation analysis previously mentioned. A schematic diagram of solvent separation procedure is shown in Figure 5. The solvent separation is performed as follows:

1. Wash the reactor with 150 ml of THF solvent to recover the reaction products (liquid + solid) from the reactor.

2. Immerse the centrifuge tube containing the reaction products plus THF for 10 minutes in a ultrasonic bath containing water.

3. Centrifuge the sample at 3000 rpm for 15 minutes.

4. After centrifugation, the solvent and soluble products are decanted into 500 ml flasks previously labeled with the run number.

5. Steps 1 through 4 are repeated three times with

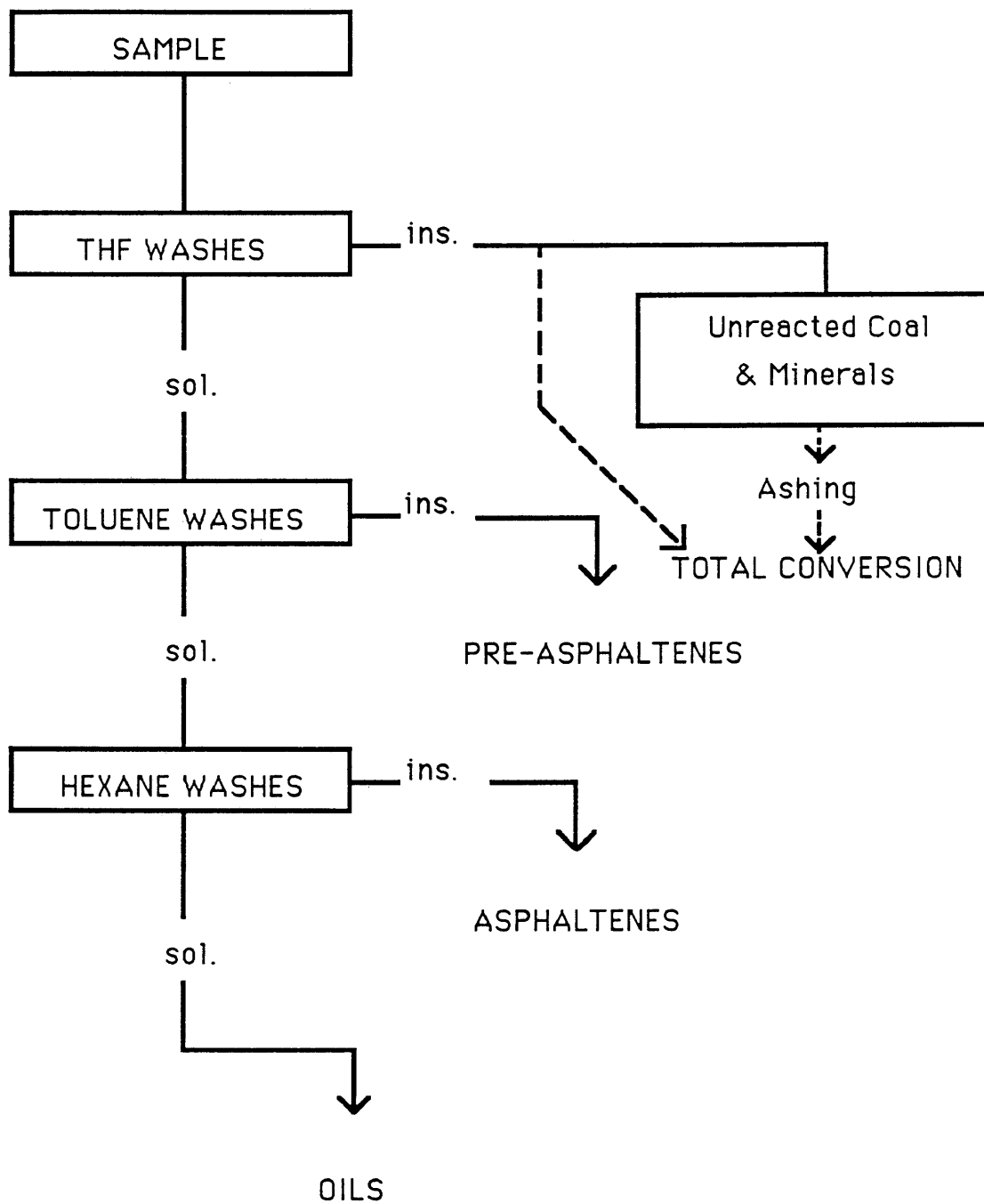


Figure 5. Schematic of Solvent Separation Procedure

fresh THF, to insure complete removal of THF solubles.

6. The centrifuge tubes containing the residue are dried over-night at 100°C, and then weighed to a precision of 0.01 grams to determine the weight of "THF insolubles".

7. The THF washes (THF + soluble products) are evaporated at 80°C and 1 atm in a rotary evaporator to separate the THF solvent from the reaction products.

8. Steps 2 through 6 are repeated using toluene and the THF soluble material separated in step 7 to determine the weight of "toluene insolubles".

9. The toluene washes are then evaporated in a rotary evaporator to separate toluene solvent at 50°C under vacuum.

10. Steps 2 through 6 are again repeated using hexane solvent with the "toluene soluble" material separated in step 9, to determine the weight of "hexane insoluble" product.

4. EXPERIMENTAL DESIGN

4.1 Basic Argument

As cited in an earlier discussion, extra care is required to determine the intrinsic rate of chemical reaction in the absence of other confounding rate effects. This is done by eliminating side-effects, such as those imposed when using a hydrogen donor solvent. As evidenced by many researchers, different hydrogen donor solvents have different hydrogen donor abilities which can affect the conversion level and intrinsic conversion rate of a particular coal due to differing rates of hydrogen transfer from the donor vehicle (26). For this reason, a non-hydrogen donor solvent was preferred as the reaction system vehicle. For the reactions performed with a non-hydrogen-donor vehicle, the role of the vehicle is to aid in dissolving the liquid products and to reduce the viscosity of the liquid products, allowing the recovery to be performed more easily.

However, using molecular hydrogen as a hydrogen source in coal liquefaction is questionable since the hydrogen molecule has a strong bond energy (104 Kcal/mole H₂). Thus the mechanism of hydrogen gas as a hydrogen source, and the different roles between the hydrogen-donor solvents and molecular hydrogen gas in different surroundings should be further discussed. Vernon (64) studied the role of hydrogen

gas as a hydrogen source using dibenzyl and diphenyl as model compounds (which are suitable representatives of strong and weak carbon-carbon bonds in coal). Product yields (benzene, ethylbenzene, and its ratio) were compared between reaction with tetralin only and reaction with tetralin and hydrogen gas. Vernon reported that the ratio of benzene/ethylbenzene was much higher in the presence of gas phase molecular hydrogen than when compared to the system of tetralin only. Thus it can be concluded that hydrogen gas serves as a hydrogen source in the presence of a radical initiator. Vernon's results support the hypothesis that hydrogen gas helps cleave strong bonds in coal by attacking those bonds. In summary, hydrogen gas can act as a homogeneous hydrogen-donor, meaning that its functionality during the reaction is directly influenced by the chemical properties of a coal.

4.2 Detailed Experimental Matrix

The following experimental design matrices were planned in order to satisfy the objectives of this research. In this research, identically equal reaction and separation techniques were used as with Shin (23), who previously used the same reactor system. Thus, the data from this work could be appended to Shin's results, providing a larger data base in order to correlate kinetic parameters with coal properties.

* Stage 1. Measurement of Rate Data

- Coals : 5 Penn State Coals
- Solvent : Aromatic (1-MN)
- Reaction times : 3, 5, 10, 15, 40 min
- Reaction temperatures: 375, 400, 425°C
- Cold pressure : 900 psi (H2 gas)

* Stage 2. Kinetic Modelling

- Development and determination of the best model for all coals.

- Calculation of activation energy.

* Stage 3. Correlational Efforts

- Correlation of activation energy and kinetic parameters.

{

5. RESULTS AND DISCUSSION

5.1 Definition of Conversion

The following definition of conversion was used to calculate reaction conversion .

$$\text{Conversion(wt\%)} = \frac{\left[\begin{array}{l} \text{Organic fraction in coal converted} \\ \text{to solvent solubles by the reaction} \end{array} \right]}{\left[\text{Total organic fraction in coal} \right]} \times 100$$

By assuming that the amount of mineral matter in coal does not change during the reaction and that the amount of mineral matter can be represented by the amount of ash measured by Penn State Coal Bank, the following relations can be developed:

$$\left[\begin{array}{l} \text{Total organic fraction} \\ \text{in coal} \end{array} \right] = \text{Total coal} - (\text{Ash amount} + \text{Moisture content})$$

$$\left[\begin{array}{l} \text{Organic fraction con-} \\ \text{verted by reaction only} \end{array} \right] = \text{Solvent solubles} - \left[\begin{array}{l} \text{Intrinsic} \\ \text{solubles} \end{array} \right]$$

Solvent solubles = Dry coal - Solvent insolubles(dry)

Intrinsic solubles = Solubility of coal in a solvent at room temperature without reaction

$$\text{Conversion(wt\%)} = \frac{(D - SI) - I}{T - (A + M)} \times 100$$

Where, T = Total Coal

A = Ash amount

M = Moisture content

S = Solvent solubles

I = Intrinsic solubles

D = Dry coal

SI = Solvent insolubles (Dry)

The intrinsic solubilities in toluene and THF for the 5 coals studied were obtained from separation analysis at room temperature. These were found to be very small (2-5 wt%) and were subsequently neglected since these values were in the range of experimental error.

5.2 Measurement of Kinetic Data

Rate data for conversion to THF and toluene solubles were measured for the 5 Penn State coals at three different temperatures. Conversion rate data to THF and toluene solubles are shown graphically in Figures 6 through 15. Numerical data for these figures are tabulated in Appendix 1. As can be seen from Figures 6 through 10, conversion to THF solubles was relatively rapid compared to conversion to toluene solubles. Conversion to THF solubles for Weir

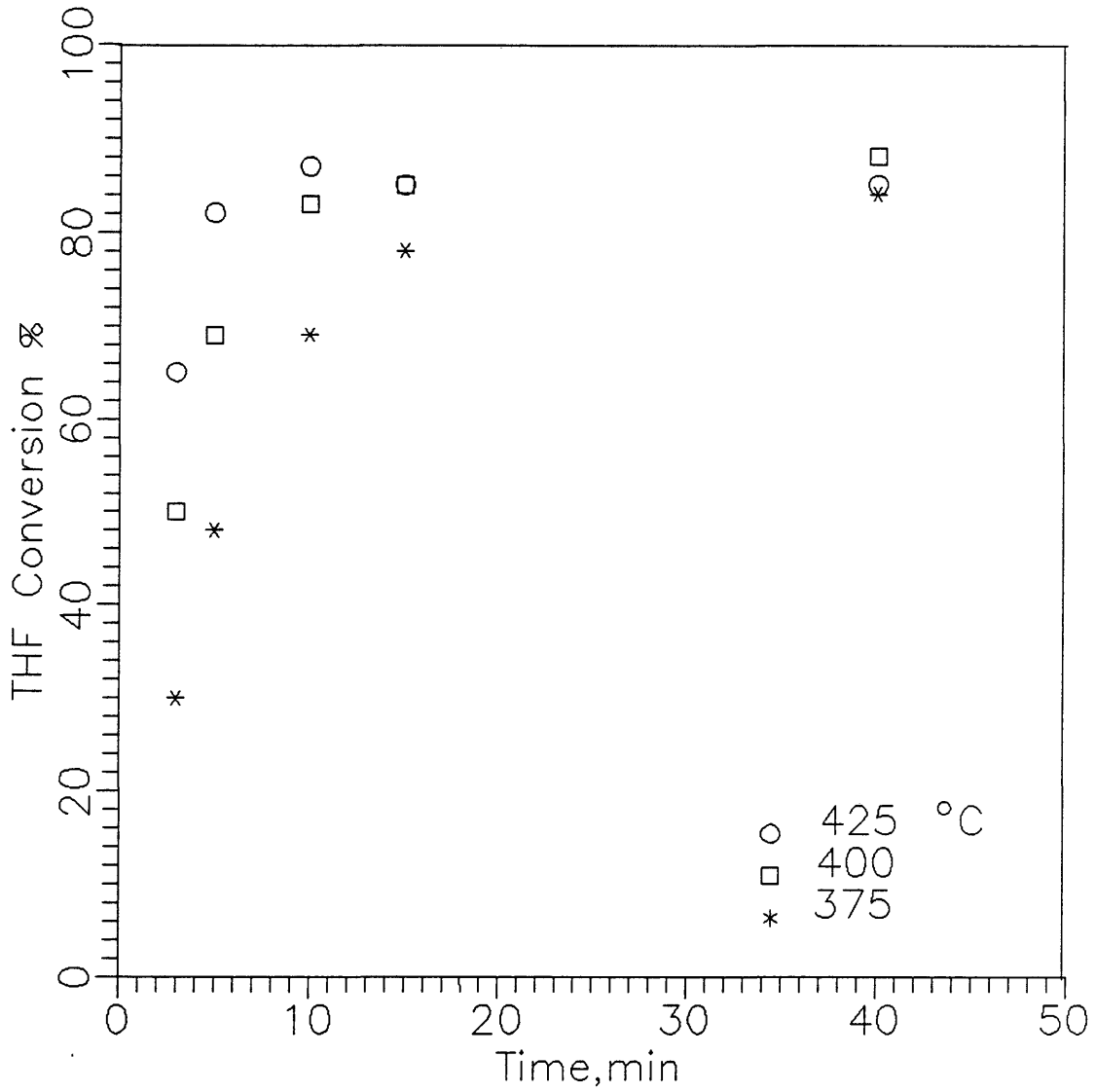


Figure 6. Conversion to THF solubles vs. Time

Coal : Weir Pittsburg

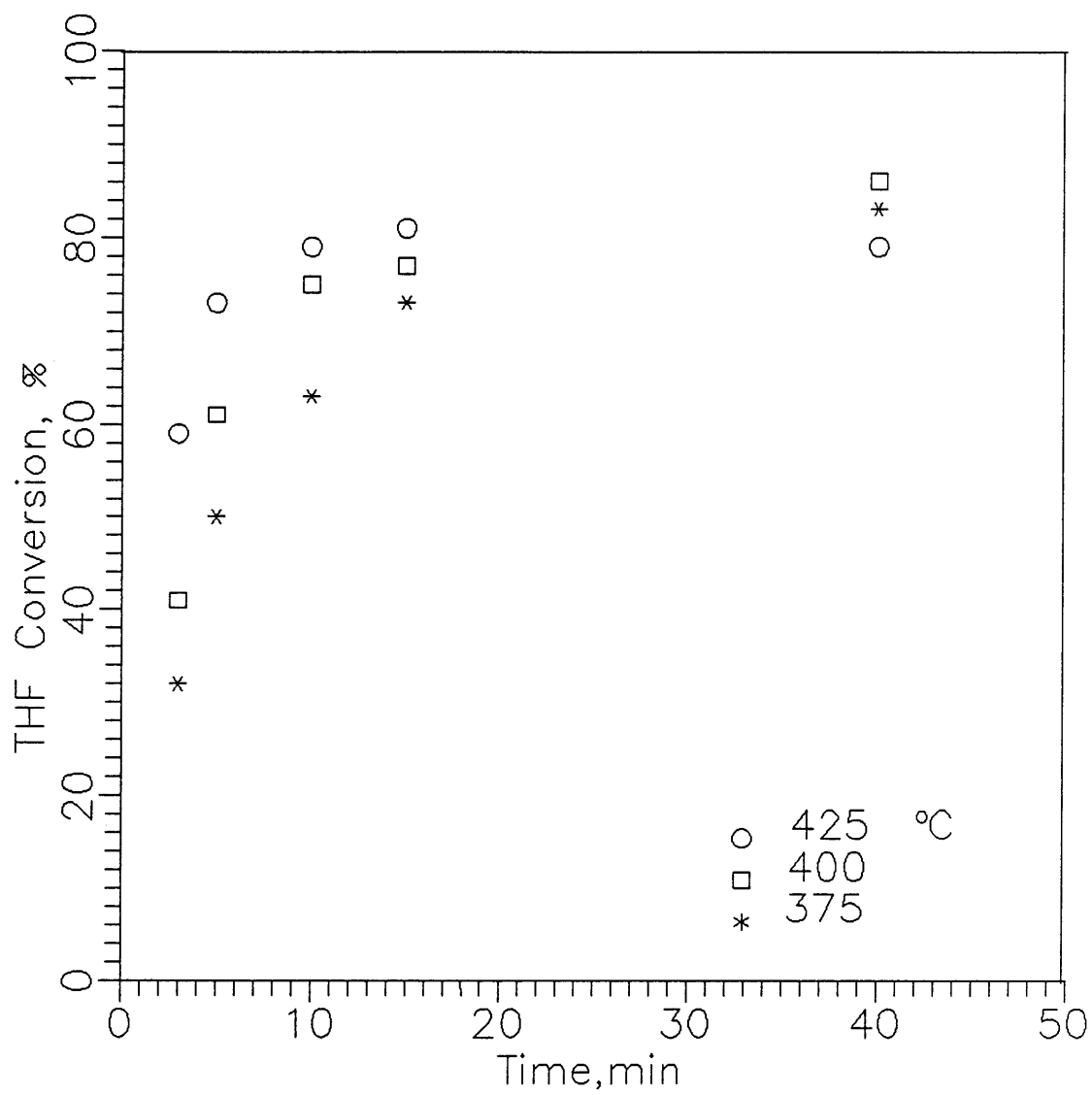


Figure 7. Conversion to THF solubles vs. Time

Coal : Bevier-Wheeler

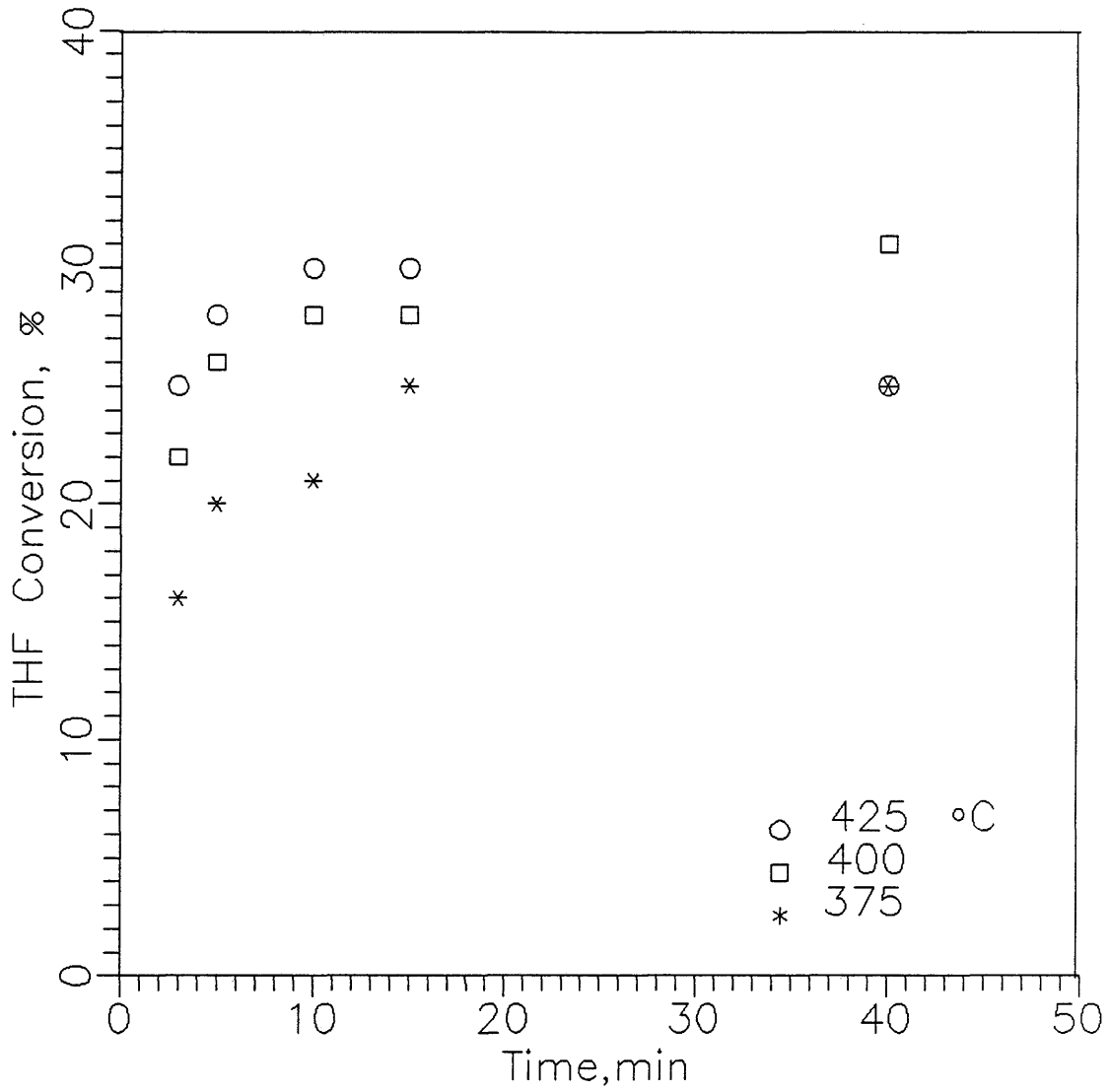


Figure 8. Conversion to THF solubles vs. Time

Coal : Lower Freeport

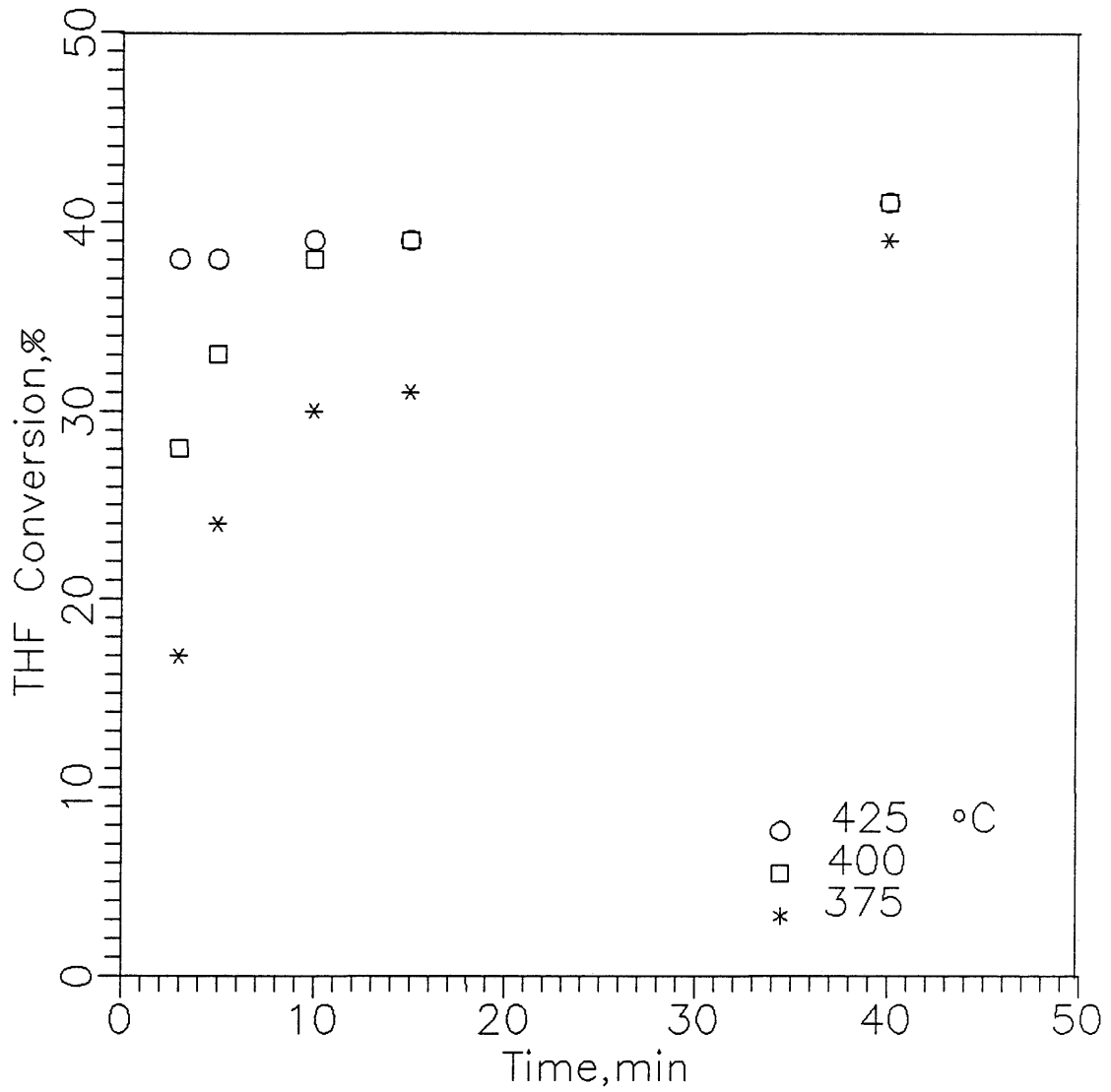


Figure 9. Conversion to THF solubles vs. Time

Coal : Lower Sudduth

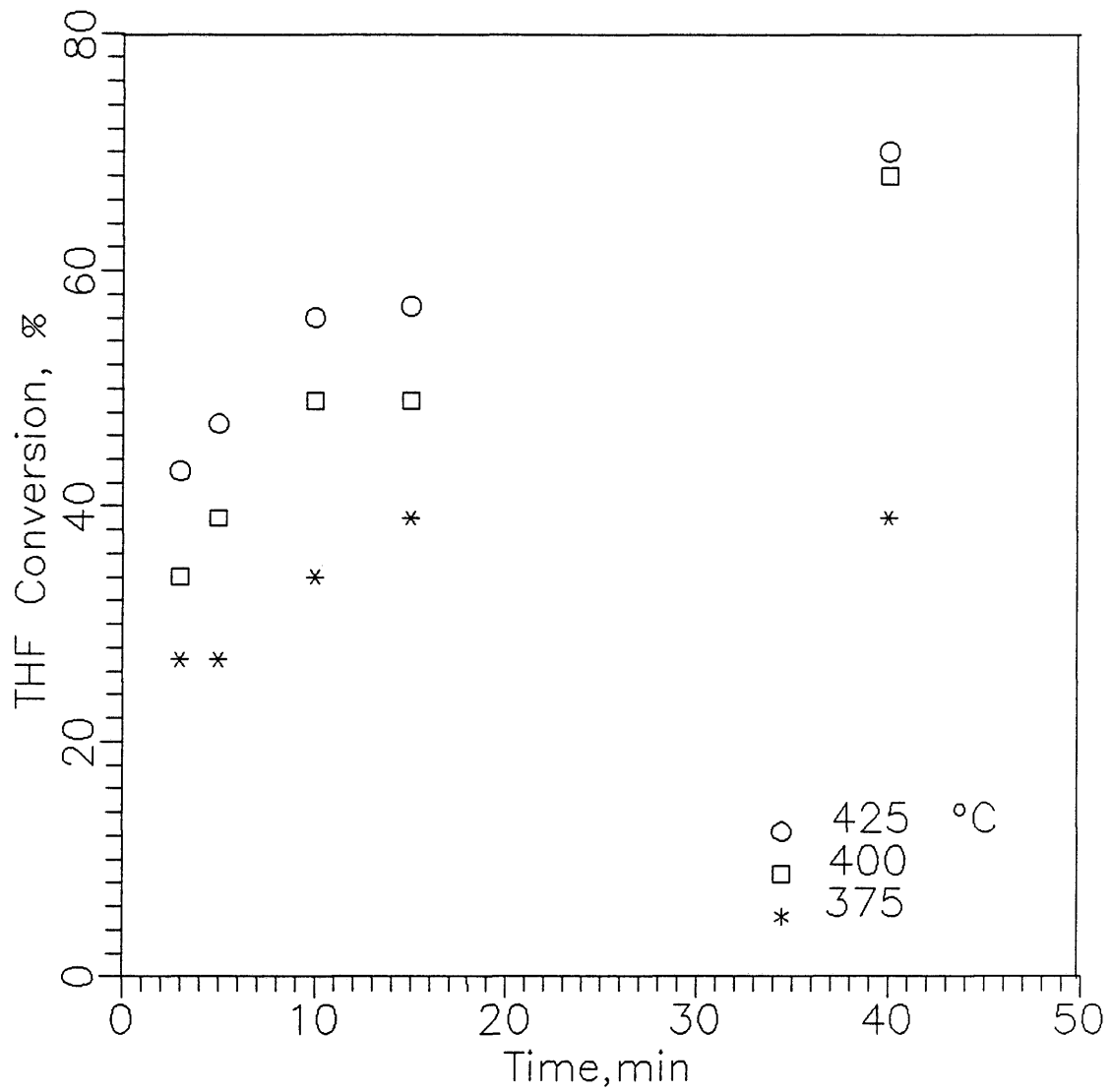


Figure 10. Conversion to THF solubles vs. Time

Coal : Splashdam

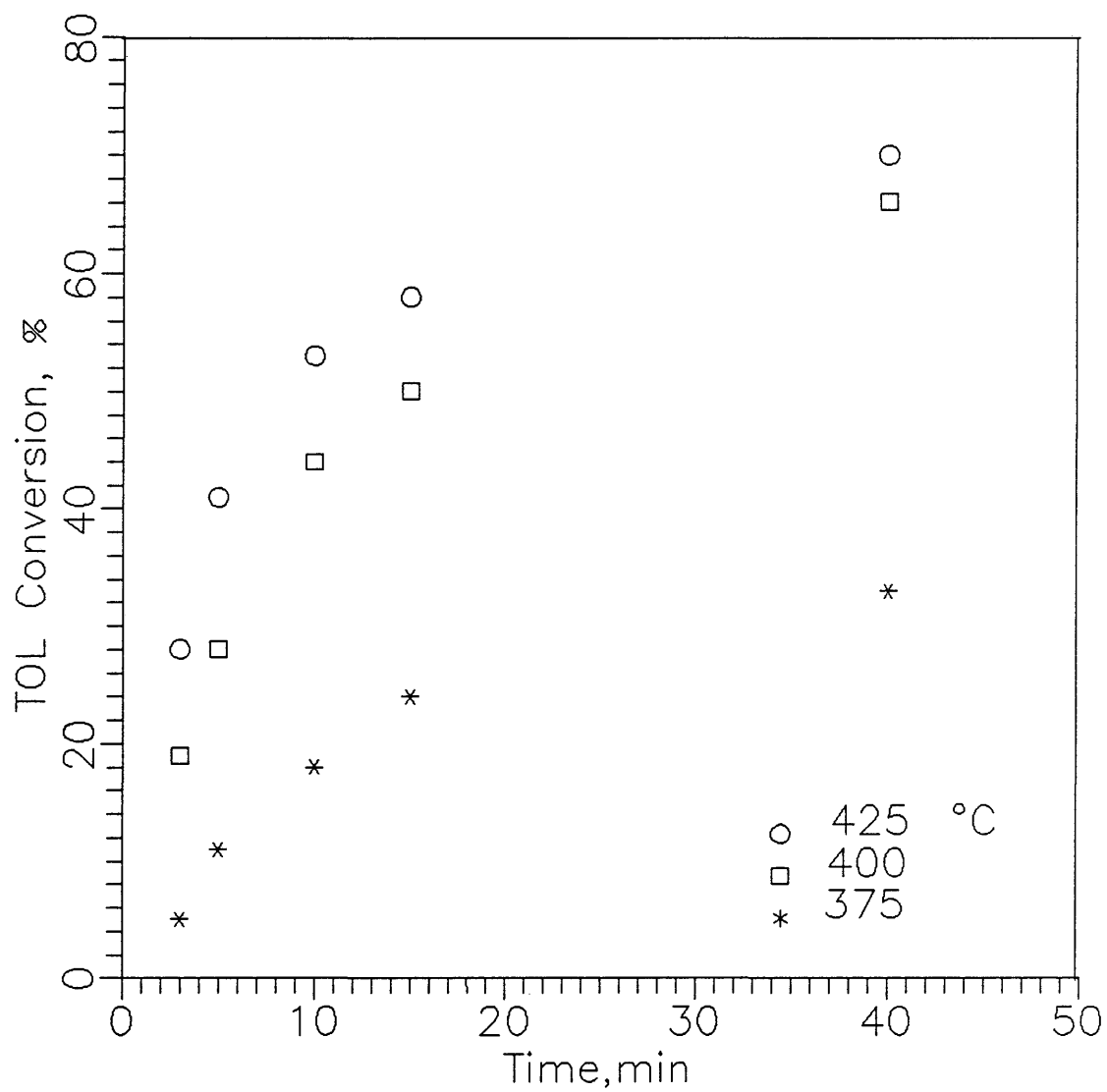


Figure 11. Conversion to Toluene solubles vs. Time

Coal : Weir Pittsburg

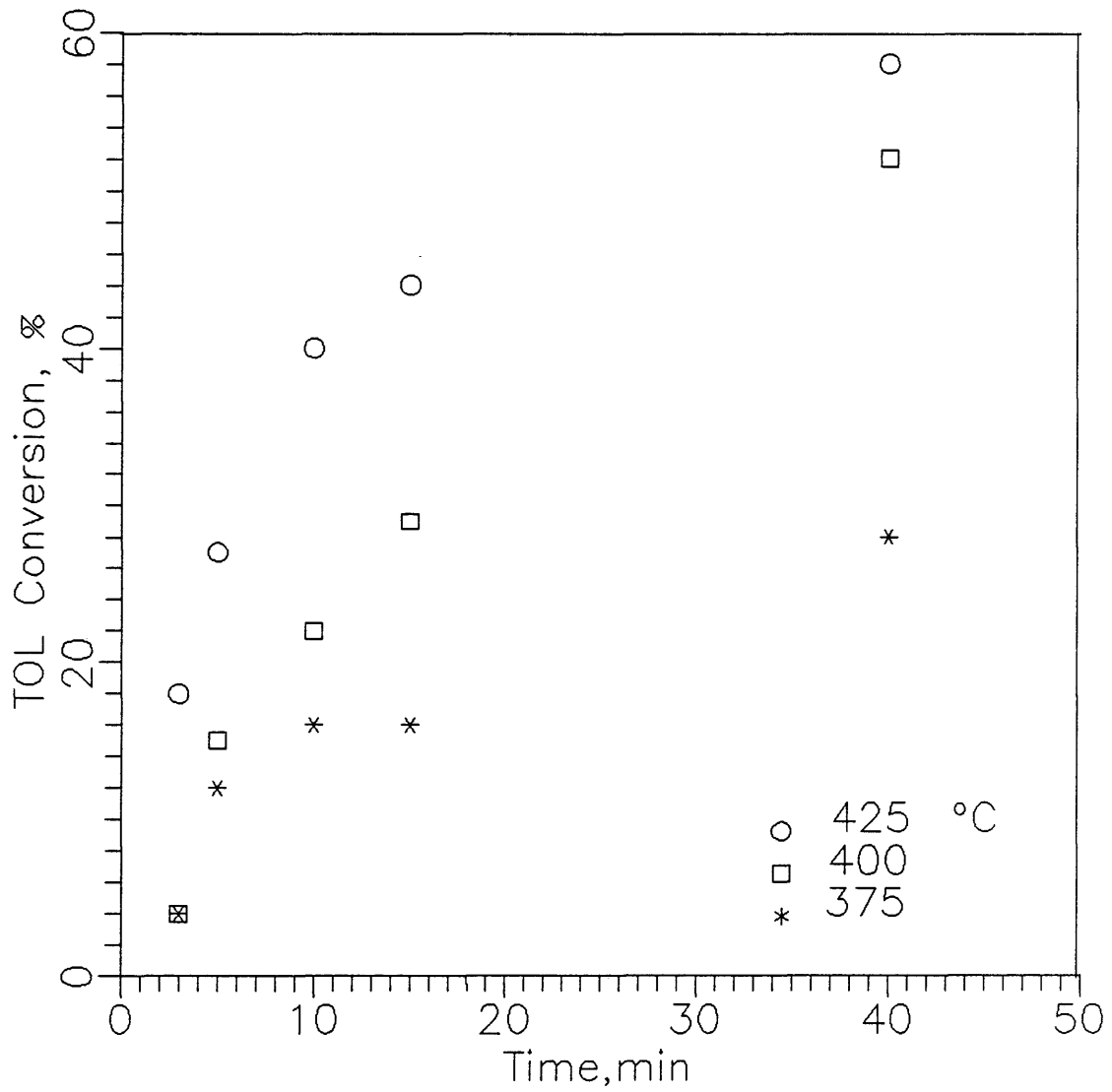


Figure 12. Conversion to Toluene solubles vs. Time

Coal : Bevier-Wheeler

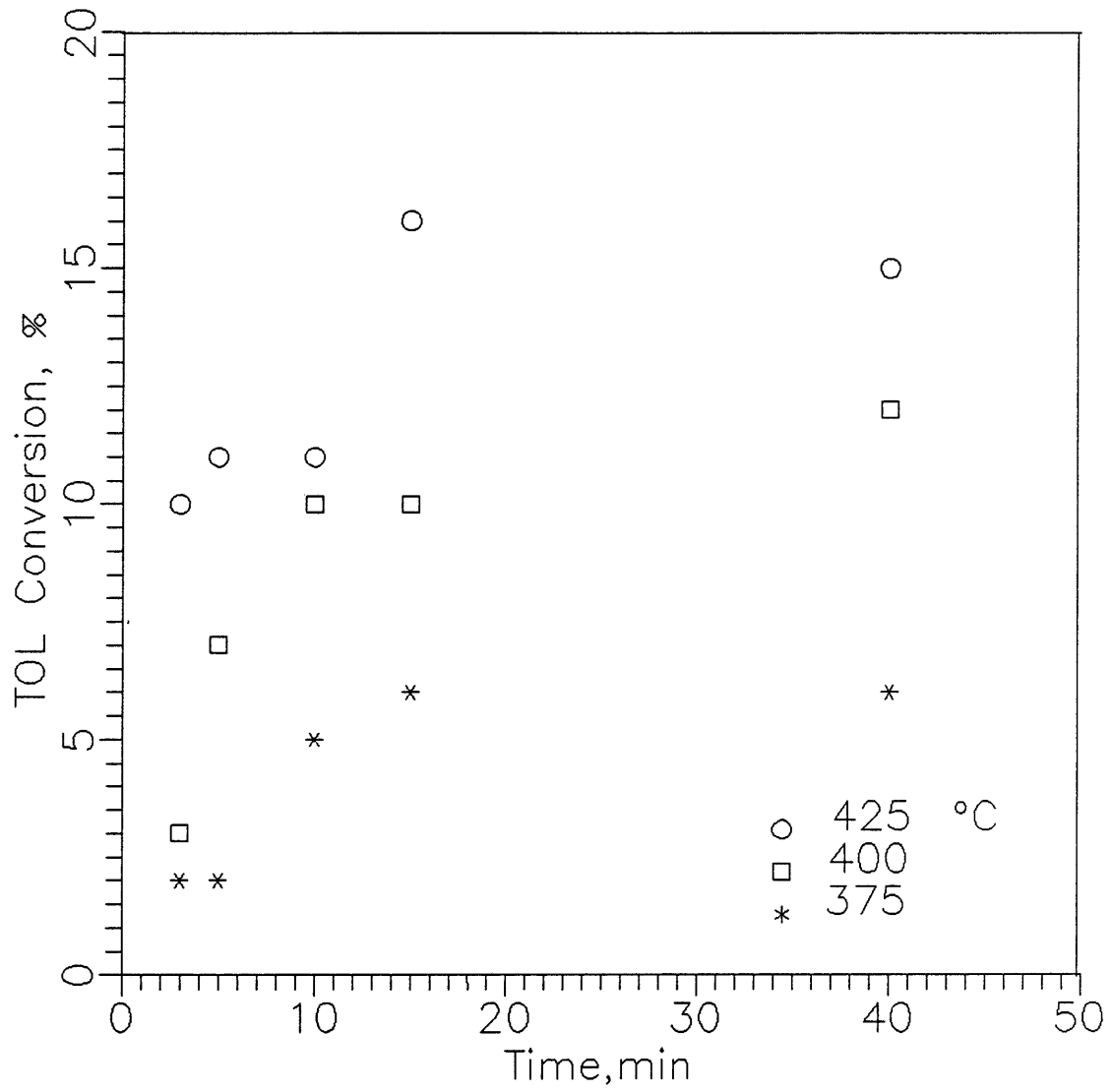


Figure 13. Conversion to Toluene solubles vs. Time

Coal : Lower Freeport

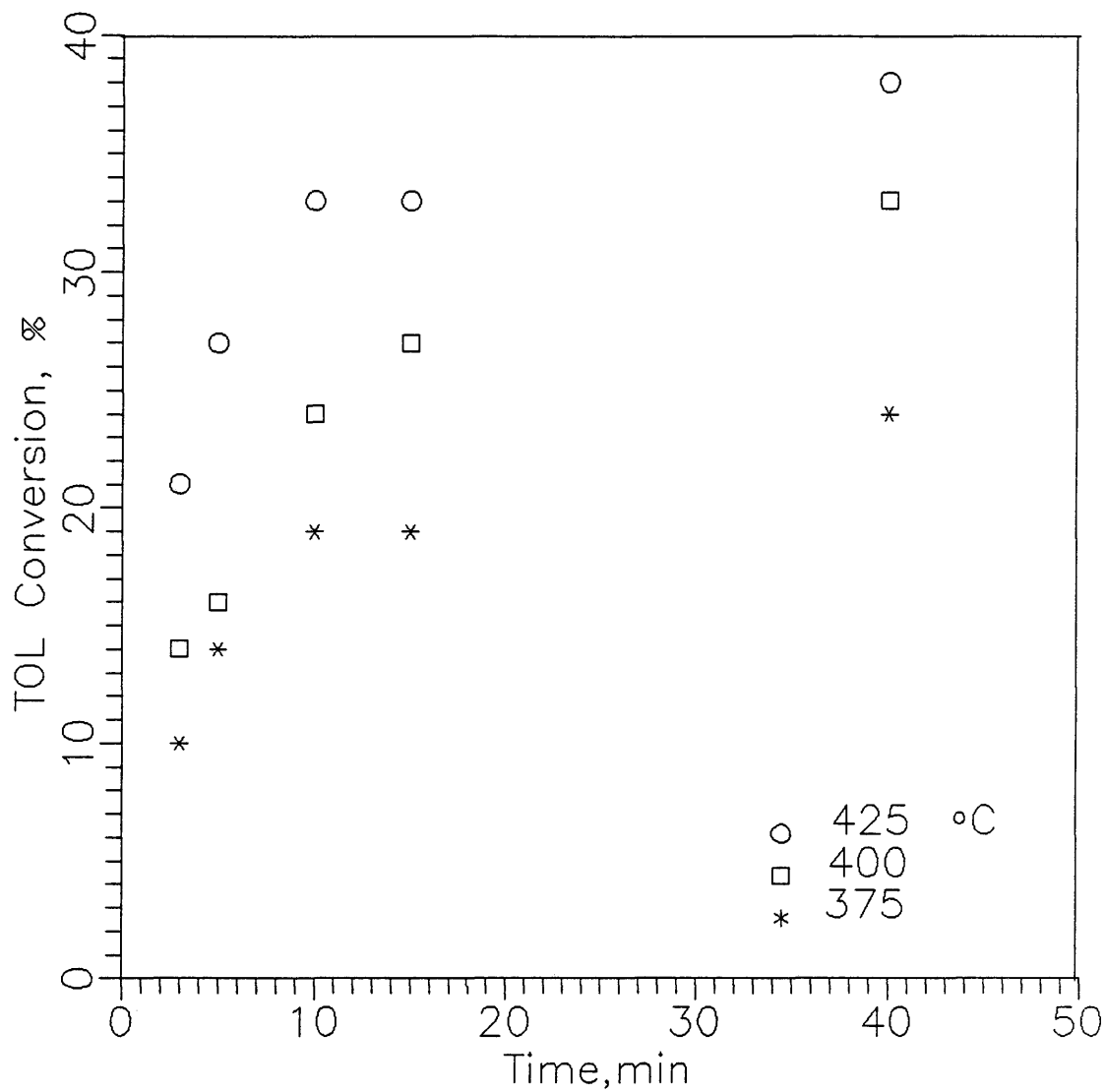


Figure 14. Conversion to Toluene solubles vs. Time

Coal : Lower Sudduth

ARTHUR LAKES LIBRARY
COLORADO SCHOOL of MINES
GOLDEN, COLORADO 80401

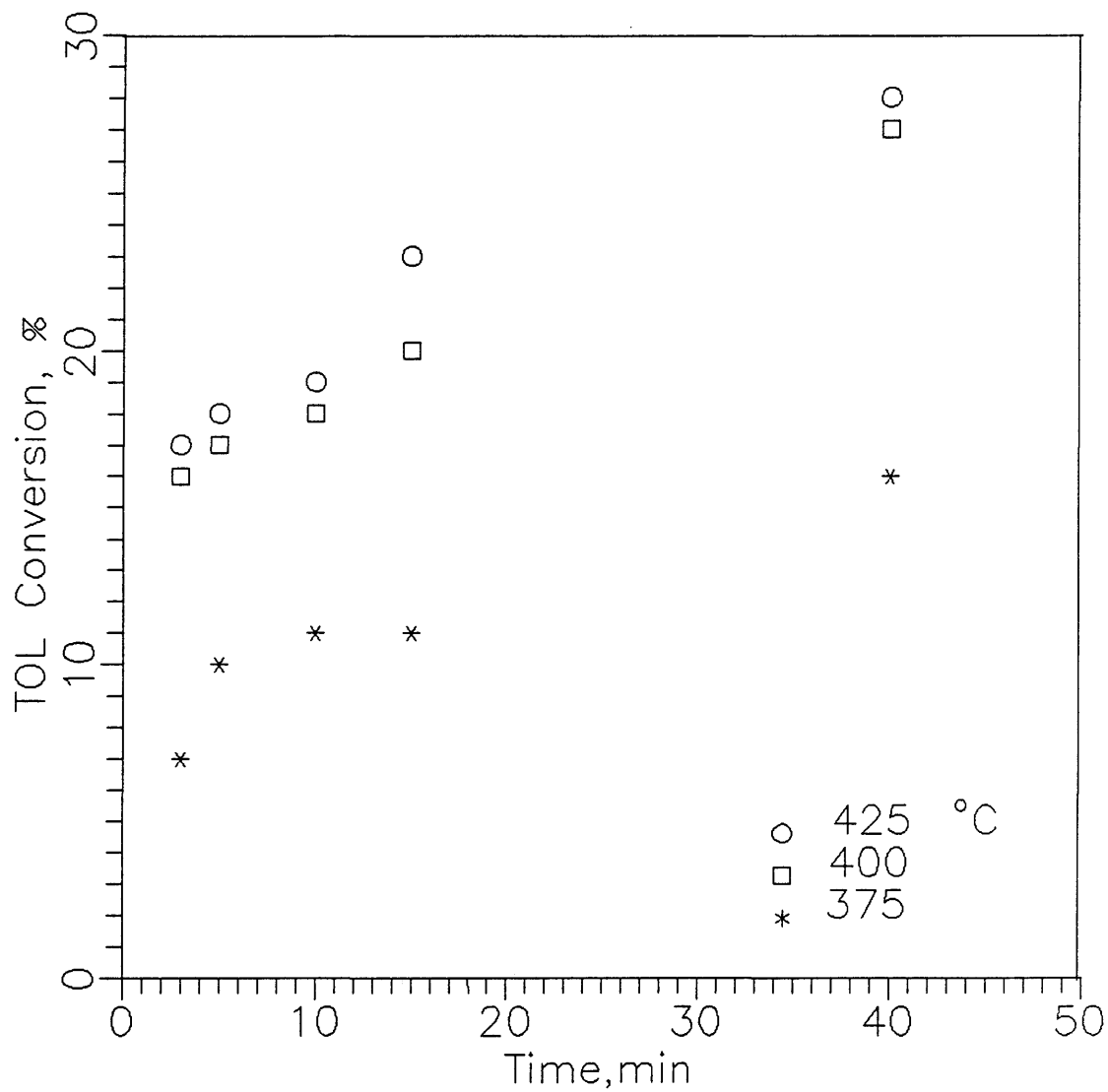


Figure 15. Conversion to Toluene solubles vs. Time

Coal: Splashdam

Pittsburg, Bevier-Wheeler, Lower Freeport, and Lower Sudduth coals (Figures 6, 7, 8, 9) shows almost the expected behavior, in that the conversion reaches an equilibrium value in early stages of the reaction for high reaction temperatures (425°C). For Splashdam coal (Figure 10) conversion to THF solubles increases continuously during the reaction at high temperature. Regressive reactions introducing reversibility into the data become more appreciable at higher reaction temperature as seen in Figures 6 through 10. It is known that this reversible (regressive) reaction is caused by a recombination of primary free radicals initially produced thermally from coal. Conversion data to THF solubles show that reversible reactions start dominating at higher temperature (425°C). This behavior can be correlated to the free swelling index of the coal, as shown in Table 3. The swelling index reflects the degree of cross-linking in coal, i.e. as the free swelling index decreases, the degree of cross-linking increases (47). As noted previously, these linking bonds will be more rapidly and completely cleaved thermally at higher temperature. From this reasoning coal with a higher cross-linking density will produce more primary radicals that will in turn recombine if they are not quenched rapidly. The radical quenching rate is much slower in an aromatic vehicle (1-MN) than in a donor vehicle (tetralin). As a result reversible reactions are much more

Table 3. Free Swelling Index of Coals

Coal	Free Swelling Index
Splashdam	8.0
Weir-Pittsburg	5.5
Bewier-Wheeler	5.0
Lower-Freeport	1.0
Lower-Sudduth	0.0

likely to occur in an aromatic solvent.

5.3 Kinetic Modelling

Measured kinetic data for 5 coal samples from Penn State Coal Bank were fitted to various kinds of kinetic models tabulated in Table 4. As a data fitting criteria, standard error of estimate values (SEE) were calculated for each model, and these values are presented in Table 5 for THF solubles, and in Table 6 for toluene solubles. The following definition of SEE was used.

$$SEE = \frac{\sqrt{\sum^n (X - X^*)^2}}{n}$$

where, X = experimental values of coal conversion (wt%)

X* = estimated values of coal conversion by the model (wt%)

n = the number of data points

To calculate the values of standard error of estimate (SEE) for a particular model, the procedure outlined in Table 7 was used. The computer program utilized for these calculations is presented in Appendix 3. As can be seen from Table 5, the first and second order irreversible models were least suitable for fitting the data, since the average value of

Table 4. Kinetic Models

Model	Rate Expression	integrated Form
1st order irreversible	$\frac{dx}{dt} = k(a-x)$	$x = a \left[1 - \exp(-kt) \right]$
2nd order irreversible	$\frac{dx}{dt} = k(a-x)^2$	$x = \frac{ka^2 t}{kta + 1}$
1st order reversible	$\frac{dx}{dt} = k_f(a-x) - k_r x$	$x = x_e \left[1 - \exp(-k_f a t / x_e) \right]$
2nd order reversible	$\frac{dx}{dt} = k_f(a-x)^2 - k_r x^2$	see appendix
1st-2nd order reversible	$\frac{dx}{dt} = K_f(a-x) - k_r x^2$	see appendix

Where, X = Coal conversion (d.a.f basis, wt%)

x_e = Equilibrium conversion (d.a.f basis, wt%)

a = Ultimate conversion (d.a.f basis, wt%)

k = Kinetic constant (k_f = forward, k_r = reverse)

t = Reaction time (minute)

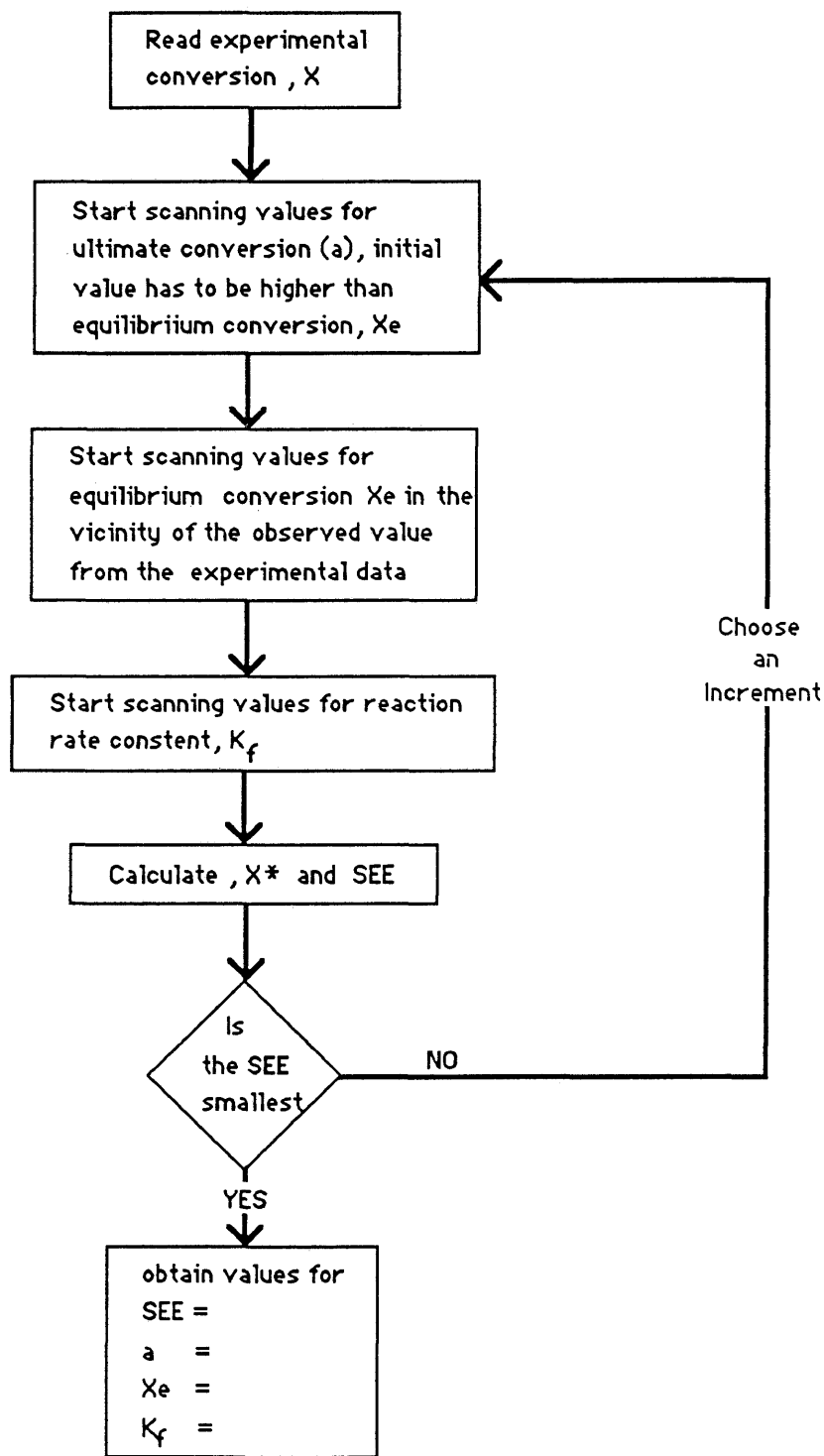
Table 5. Statistical Comparison of Kinetic Models
(THF Solubles)

Coal	Temp	First Irr.	Sec. Irr.	First Rev.	Sec. Rev.	F-S. Rev.
Weir	425	1.24	1.81	0.82	1.8	0.81
	400	0.7	2.32	0.52	2.34	0.5
	375	1.1	2.67	0.62	2.59	0.58
Bevier	425	2.28	1.4	0.4	1.15	0.38
	400	1.56	2.01	1.18	2.02	1.22
	375	1.69	1.61	1.11	1.62	1.16
Low.Sud	425	1.05	0.54	0.48	0.38	0.44
	400	0.84	0.3	0.43	0.32	0.44
	375	1.54	0.49	0.97	0.5	1
Splash.	425	2.97	1.33	2.23	1.3	2.28
	400	2.91	1.52	2.71	1.75	2.81
	375	5.9	3.93	1.14	1.12	1.27
Low.Fre	425	1.03	0.32	0.47	0.31	0.47
	400	1.51	1.28	0.84	0.86	0.85
	375	1.7	0.95	0.76	0.46	0.58
SEE=		1.868	1.499	0.979	1.235	0.986

Table 6. Statistical Comparison of Kinetic Models
(TOL Solubles)

Coal	Temp.	Fir.Irr	Sec.Irr.	Fir.Rev	Sec.rev	F-S.rev
Weir	425	1.46	1.34	1.19	1.3	1.23
	400	1.07	1.37	0.63	1.33	0.68
	375	2.13	5.61	0.41	1.4	0.33
Bevier	425	0.9	1.43	0.82	1.43	0.85
	400	1.01	2.18	1.05	2.18	1.08
	375	1.9	1.36	0.99	1	1.07
Low.Sud	425	1.1	0.44	0.66	0.45	0.68
	400	1.46	0.41	0.66	0.39	0.73
	375	2.52	1.48	0.54	0.49	0.61
Splash.	425	1.65	0.88	1.25	0.89	1.28
	400	1.9	1.09	1.32	1.08	1.35
	375	1.85	1.3	0.7	0.71	0.76
Low.Fre.	425	0.96	0.64	0.72	0.62	0.73
	400	0.96	0.54	0.36	0.39	0.35
	375	1.03	0.7	0.42	0.44	0.45
SEE =		1.46	1.385	0.781	0.94	0.812

Table 7. Algorithm for the Calculation of SEE



SEE was higher compared to reversible models for both THF and toluene solubles. From the five kinetic models investigated, the second order reversible model was determined to be the best. From a statistical point of view, the second order reversible model does represent conversion data to toluene solubles very well, but first order and first-second order reversible models fit conversion data to THF solubles better than the second order reversible model. Theoretically, the rate of the forward reaction should depend on the concentration of radicals produced and hydrogen atom, especially in the absence of a strong hydrogen donor vehicle. The reverse reaction should be second order since two species are involved in the recombination reaction.

Calculated activation energy, kinetic constants, ultimate conversion, and equilibrium conversion based upon second order reversible model are given in Tables 8 and 9. The Arrhenius plots for each of the five coals are given in Figures 16 and 17. Activation energies obtained vary from 15 to 46 kcal/mol for second order reversible model. This wide range of values indicates that the activation energy determined is a characteristic value of the coal. Activation energies are listed in Table 10 for each coal for three reversible models tested. The table indicates the important finding that ranking of coals with respect to reactivity using activation energy as the ranking parameter is essen-

Table 8. Activation Energy(THF Sol) and Kinetic Constants

MODEL: Second Reversible

Coal	E(kcal/m)	R-sq(%)	Freq.F (1/min)	k(kin) (1/min)	a(%)	Xe(%)
Weir	28.7	100	1.46E+07	0.014 0.007 0.003	89	87 88 88
Bevier	21.6	98.1	5.40E+04	0.0097 0.0047 0.0029	97	82 86 86
Low.Sud.	44.1	99.4	4.80E+12	0.0671 0.0174 0.0057	42	40 41 41
Splash.	15.3	96.7	3.68E+02	0.0059 0.0034 0.0025	71	70 70 38
Low.Fre.	27.7	100	2.40E+07	0.0483 0.0234 0.0103	32	28 31 25

Table 9. Activation Energy(TOL Sol) and Kinetic Constants

MODEL: Second Reversible

Coal	E(kcal/m)	R-sq(%)	Freq.F	k(kin)	a(%)	Xe(%)
Weir	36.5	95.5	1.31E+09	0.0038 0.0021 0.0005	71	70 70 35
Bevier	29.9	98.6	7.20E+06	0.0032 0.0012 0.0006	59	58 58 29
Low.Sud.	24.5	92.7	4.80E+05	0.0111 0.0041 0.0028	39	38 35 23
Splash.	22.2	88.5	1.20E+05	0.0113 0.0092 0.0033	29	28 26 14
Low.Fre.	45.9	99.9	6.40E+12	0.0233 0.0070 0.0018	17	15 12 6

Table 10. Coal ranking with respect to Activation Energy
 (TOL Solubles)
 (E, Kcal/mol)

RANK	Fir.Rev Activ. Energy	Sec.Rev Activ. Energy	F-S Rev Activ. Energy	
1	Low.Fre. 38.4	Low.Fre. 45.9	Low.Fre. 37.1	3.8
2	Weir. 26.9	Weir. 36.5	Weir. 28.9	12.5
3	Bevier 21.0	Bevier 29.9	Bevier 23.2	6.7
4	Splash 17.7	Low.Sud. 24.5	Splash 17.2	4.8
5	Low.Sud. 16.1	Splash 22.2	Low.Sud. 17.0	24.5

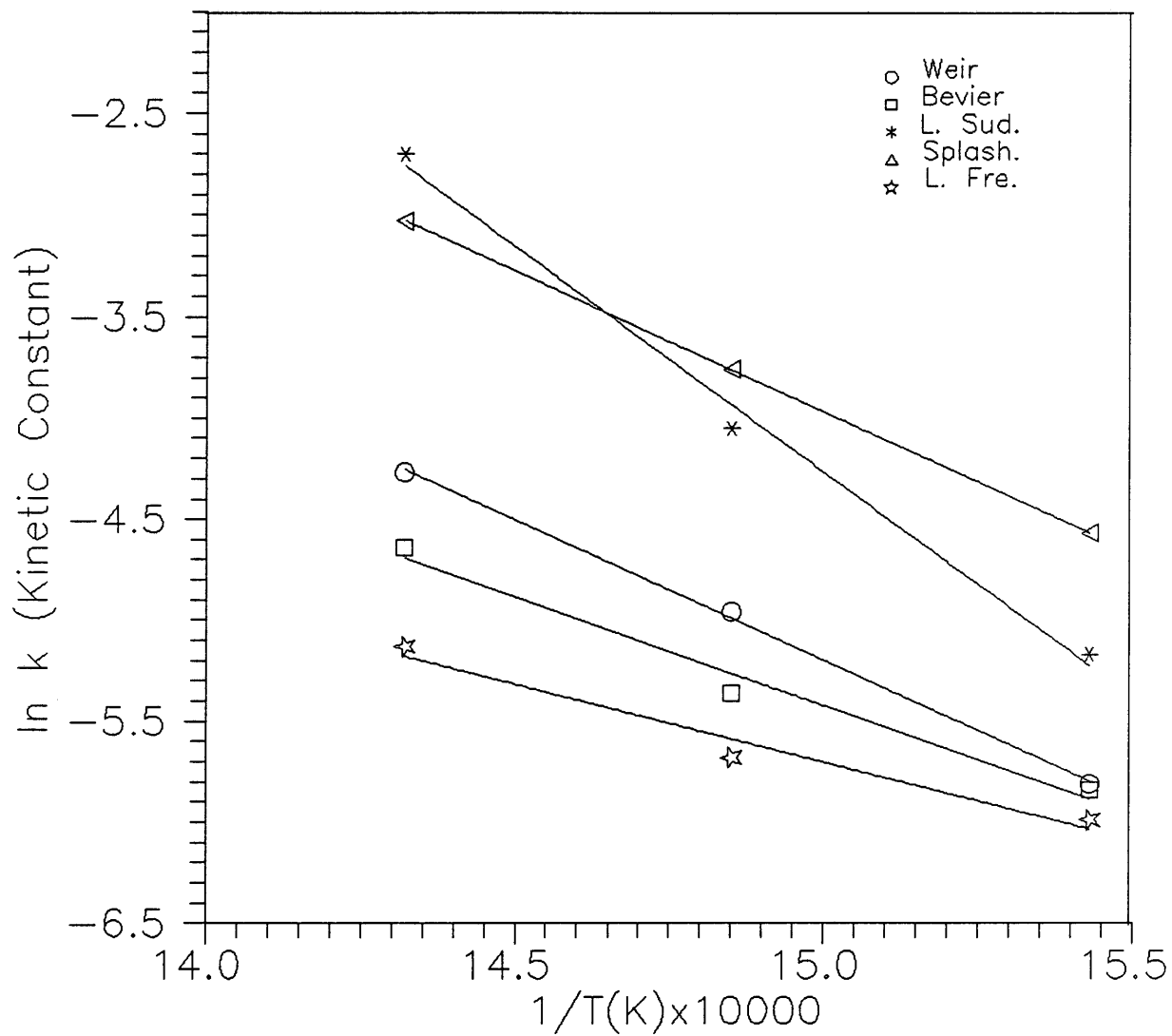


Figure 16. Arrhenius Plot (THF Solubles)

Model:Second Reversible

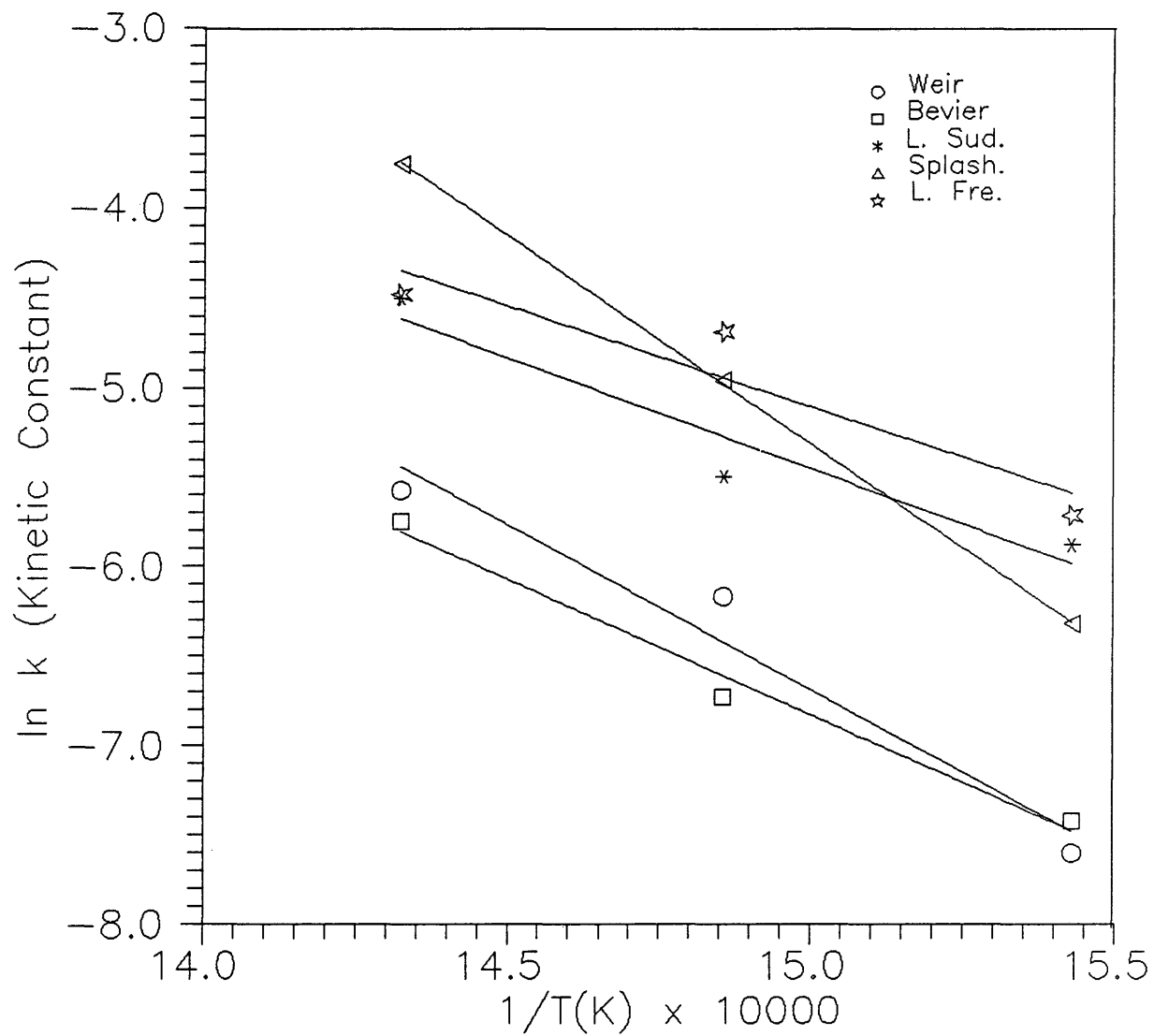


Figure 17. Arrhenius Plot (Toluene Solubles)

cially independent of the choice of kinetic model used to determine the activation energy. Irrespective of the kinetic model chosen, the coals have the same relative reactivity ranking. This finding indicates that activation energies can be used as fundamental indicators of relative reactivity.

5.4 Correlations

5.4.1 Traditional Correlations

Point-Yield Conversion

Point-yield conversions (fixed time and temperature) were first tried to correlate activation energies with coal properties by using linear regression analysis. Multiple correlation coefficients for correlations of the yield of toluene solubles with the carbon plus oxygen contents of the parent coals are presented in Table 11. As shown conversion to toluene solubles is correlated well with total carbon plus oxygen (wt%/m.w) for the 5, 10, and 15 minutes residence times at 425°C. However, at temperatures of 400 and 375°C, significantly weaker correlations were found. The weakness of the point-yield conversion technique in describing coal reactivity is also illustrated graphically in Figures 18 through 20.

Kinetic Constant

Rate constants for coal conversion to THF and toluene solubles at 425, 400, 375°C were next used as correlational

Table 11. Multiple Correlation Coefficient of
Point-Yield Conversion
(Toluene Solubles vs. Total C+O Content)

Temp (°C)	Reaction Time (min)				
	3	5	10	15	40
425	72.2	90.6	97.9	98.4	58.2
400	11.3	61.3	78.7	87.6	94.7
375	0	34.7	63.2	80.7	89.6

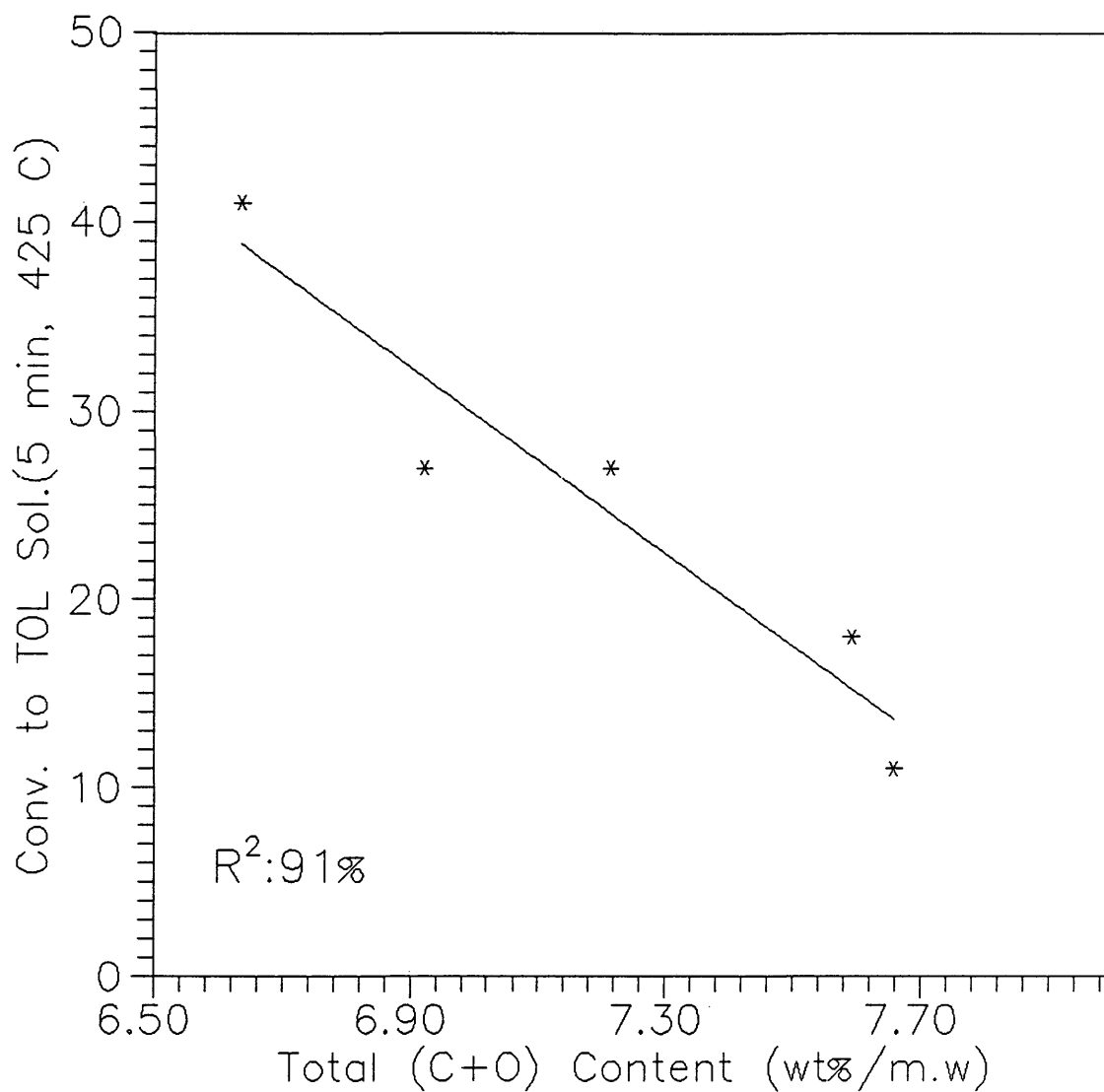


Figure 18. Conversion to Toluene Solubles vs. (C+O) Content
(5 min, 425°C)

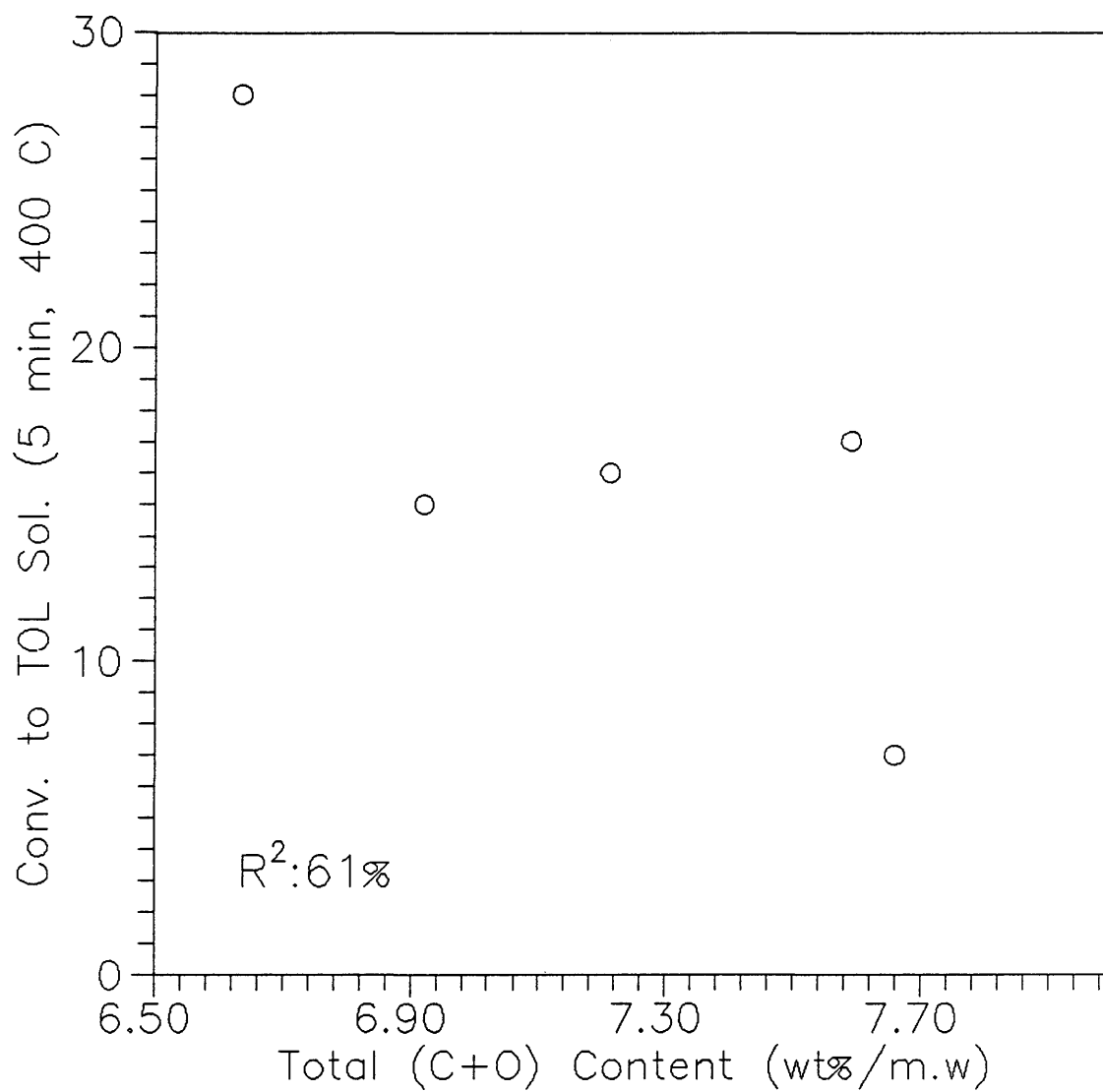


Figure 19. Conversion to Toluene Solubles vs. (C+O) Content
(5 min, 400°C)

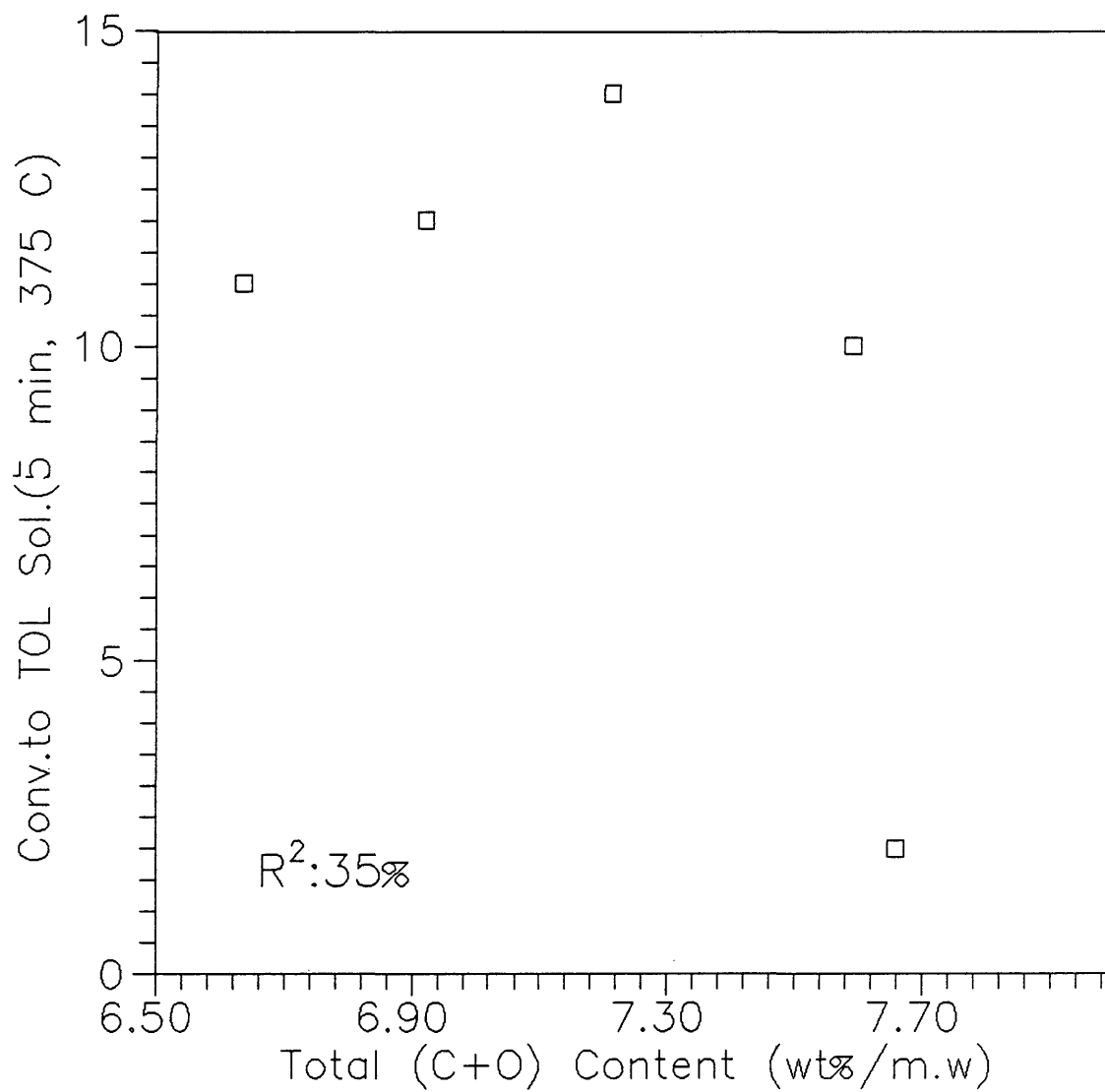


Figure 20. Conversion to Toluene Solubles vs. (C+O) Content
(5 min, 375°C)

parameters. Rate constants for conversion to toluene solubles at 425°C gave a very strong correlation (R-sq value 99%) with the total hydrogen content of the coal as shown in Figure 21. However the same strong correlations were not found at lower temperatures, as shown in Figures 22 and 23. Rate constants for conversion to toluene solubles showed progressively better correlations with total carbon plus oxygen as temperature decreased. Correlation coefficients were 72%, 81%, 83% at temperatures 425, 400, 375°C respectively.

5.4.2 Correlation of Activation Energy

Activation energy was also utilized as a reactivity definition, and correlated with coal properties such as total carbon, total hydrogen, total oxygen etc. To analyze activation energy dependence of coal properties a regression method called stepwise regression was used. This method performs a linear regression step by step to find the best subset of predictors with respect to the F-Statistic. Testing the weight of the variables, total carbon, total oxygen, total hydrogen, nitrogen and sulfur content of coal in predicting activation energy (THF solubles) was tested. The stepwise regression method determined that only carbon and hydrogen were significant (95 % confidence) in predicting activation energy for coal conversion to THF solubles. Results of this analysis are shown in Table 12. Activation

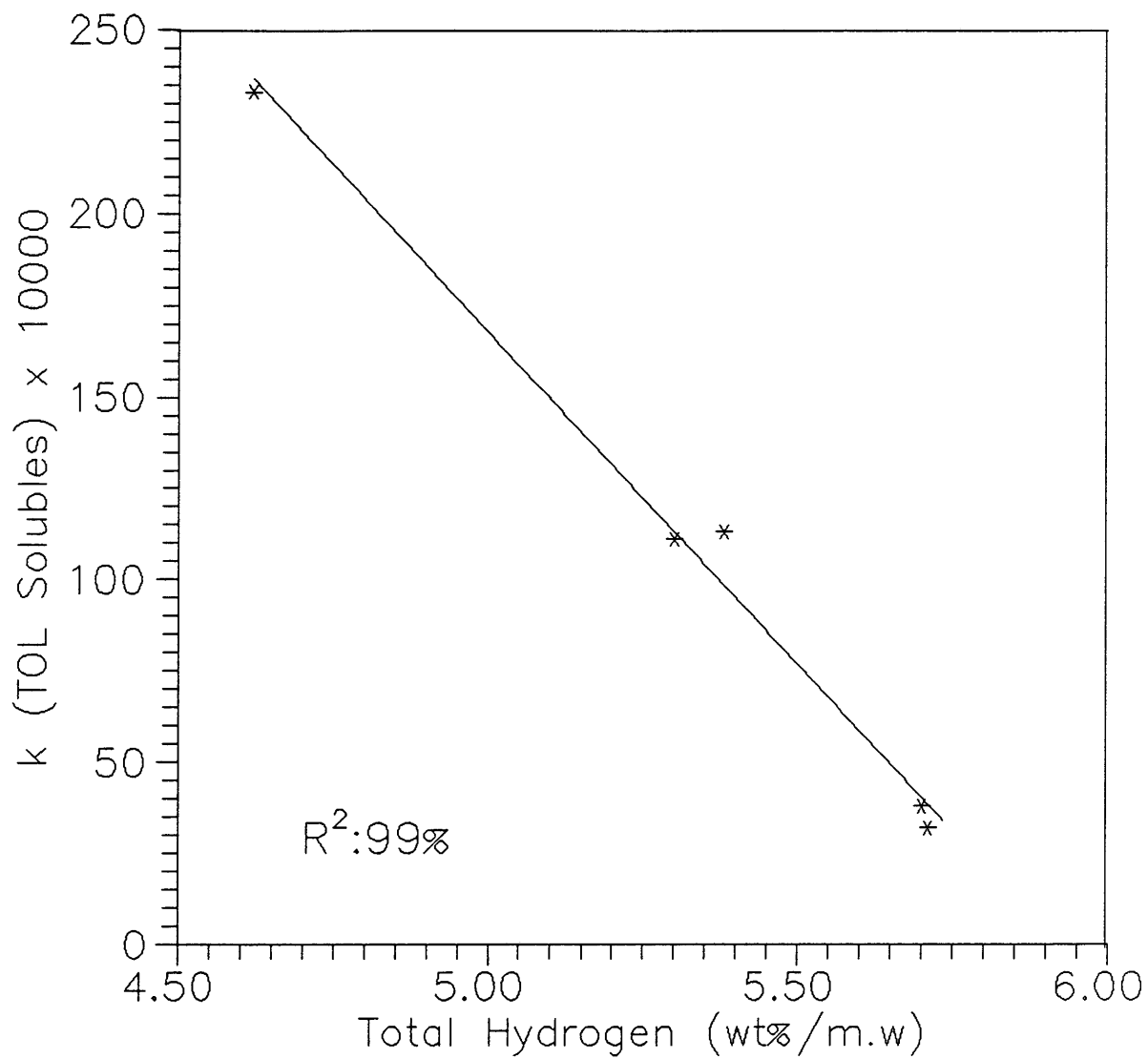


Figure 21. Correlation of Kinetic Constant (Toluene Sol.)
vs. Total Hydrogen (wt%/m.w)
Temperature: 425°C

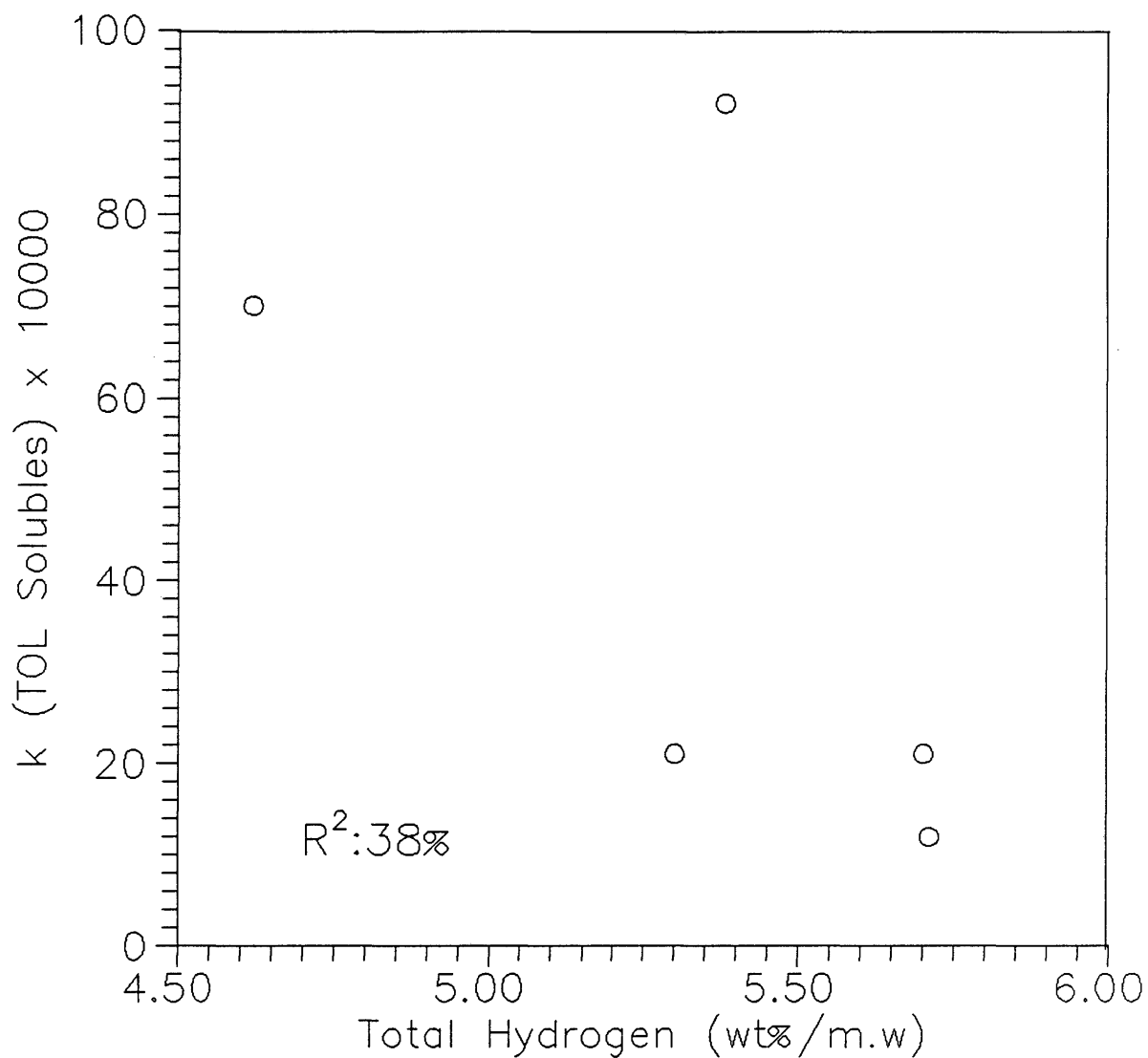


Figure 22. Correlation of Kinetic Constant (Toluene Sol.)
vs. Total Hydrogen (wt%/m.w)
Temperature: 400°C

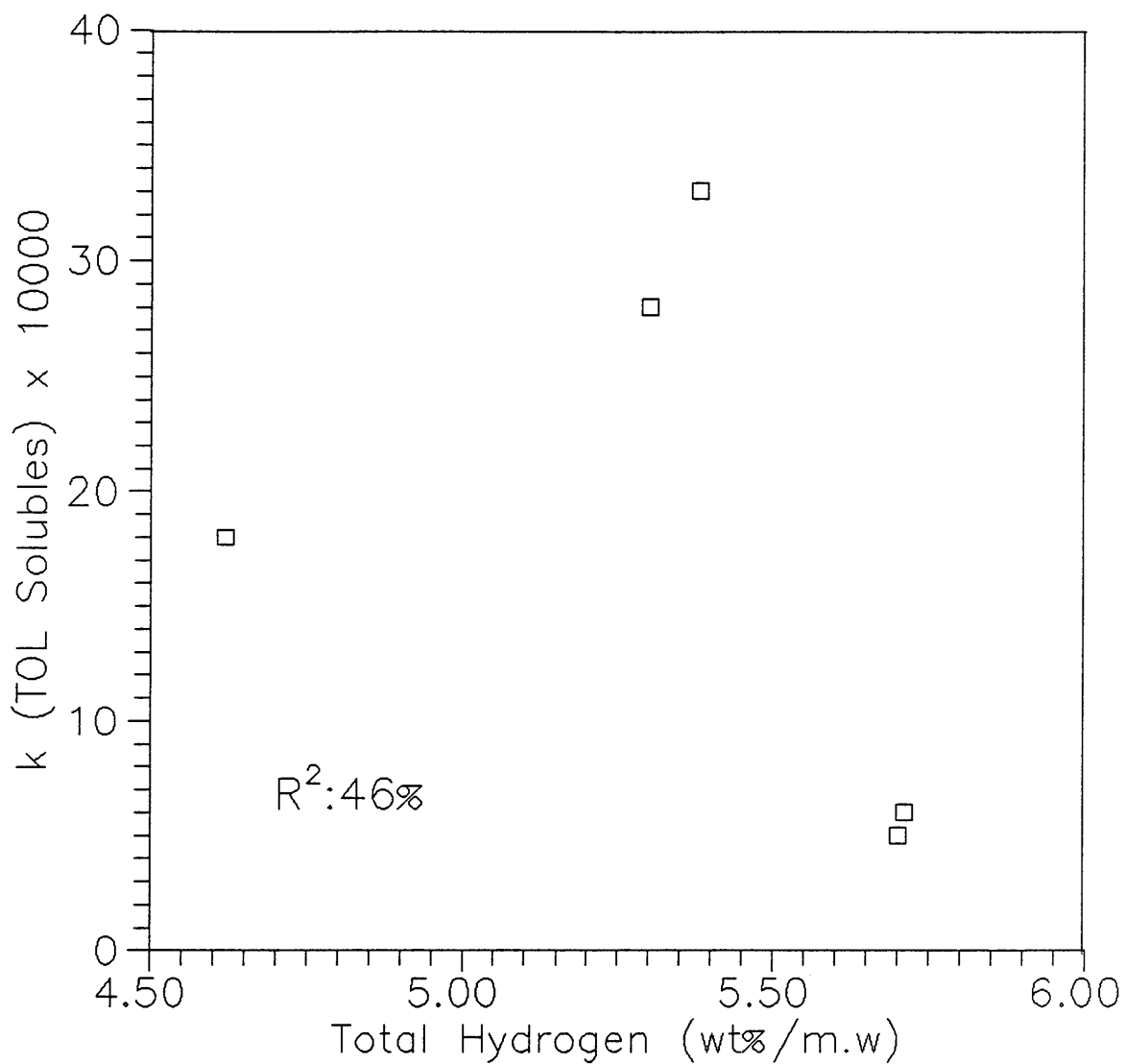


Figure 23. Correlation of Kinetic Constant (Toluene Sol.)
vs. Total Hydrogen (wt%/m.w)
Temperature: 375°C

Table 12. Stepwise Regression of Coal Properties in
Predicting Activation Energy (THF)

STEP	1	2
Constant	105.3	224.2
C%	-11.6	-16.5
T-Ratio	-2.05	-5.12
H%		-16.2
T-Ratio		-3.18
*St.dev	8.01	3.99
R-sq	58.23	93.10

*: Estimated Standard deviation of the Regression
Line.

energy for coal conversion to THF solubles was highly correlated with total carbon plus total hydrogen (R-sq 93%) and the free swelling index plus total carbon (R-sq 82%). These relationships are also illustrated in Figure 24.

$$E(\text{THF}) = 225.2 - 16.4 (C+H) \quad R\text{-sq:}93\%$$

$$E(\text{THF}) = 55.6 - 2.66 (\text{Index}+C) \quad R\text{-sq:}82\%$$

where, E = Activation energy, kcal/mole

C, H = Carbon and Hydrogen content (wt%/m.w, d.a.f)

Index= Free swelling index

Activation energy for coal conversion to toluene solubles was found to be strongly correlated with the following variables:

$$E(\text{TOL}) = 55.7 - 3.36 [I+(C*O)] \quad \{R\text{-sq:}98.1\%\}$$

$$E(\text{TOL}) = 53.8 - 3.30 [I+(H*O)] \quad \{R\text{-sq:}95.8\%\}$$

where, E = Activation energy, kcal/mole

I = Free Swelling Index

C, O, H = Carbon, Oxygen and Hydrogen content (wt%/m.w, d.a.f)

These two correlations are presented graphically in Figures 25 and 26. Frequency factor was also correlated with coal

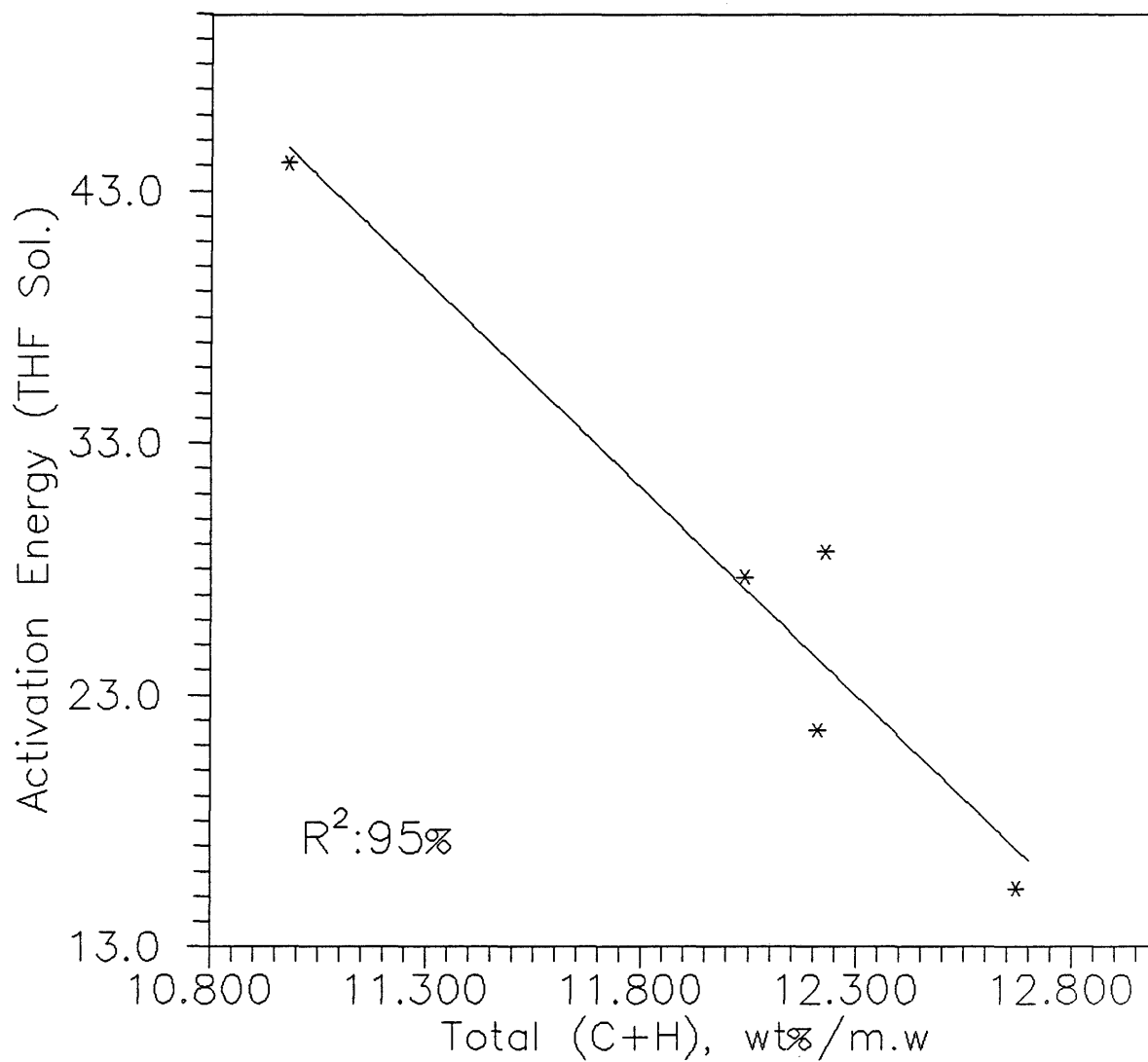


Figure 24. Correlation of Activation Energy (THF Sol.)
vs. C+H (wt%/m.w, d.a.f)

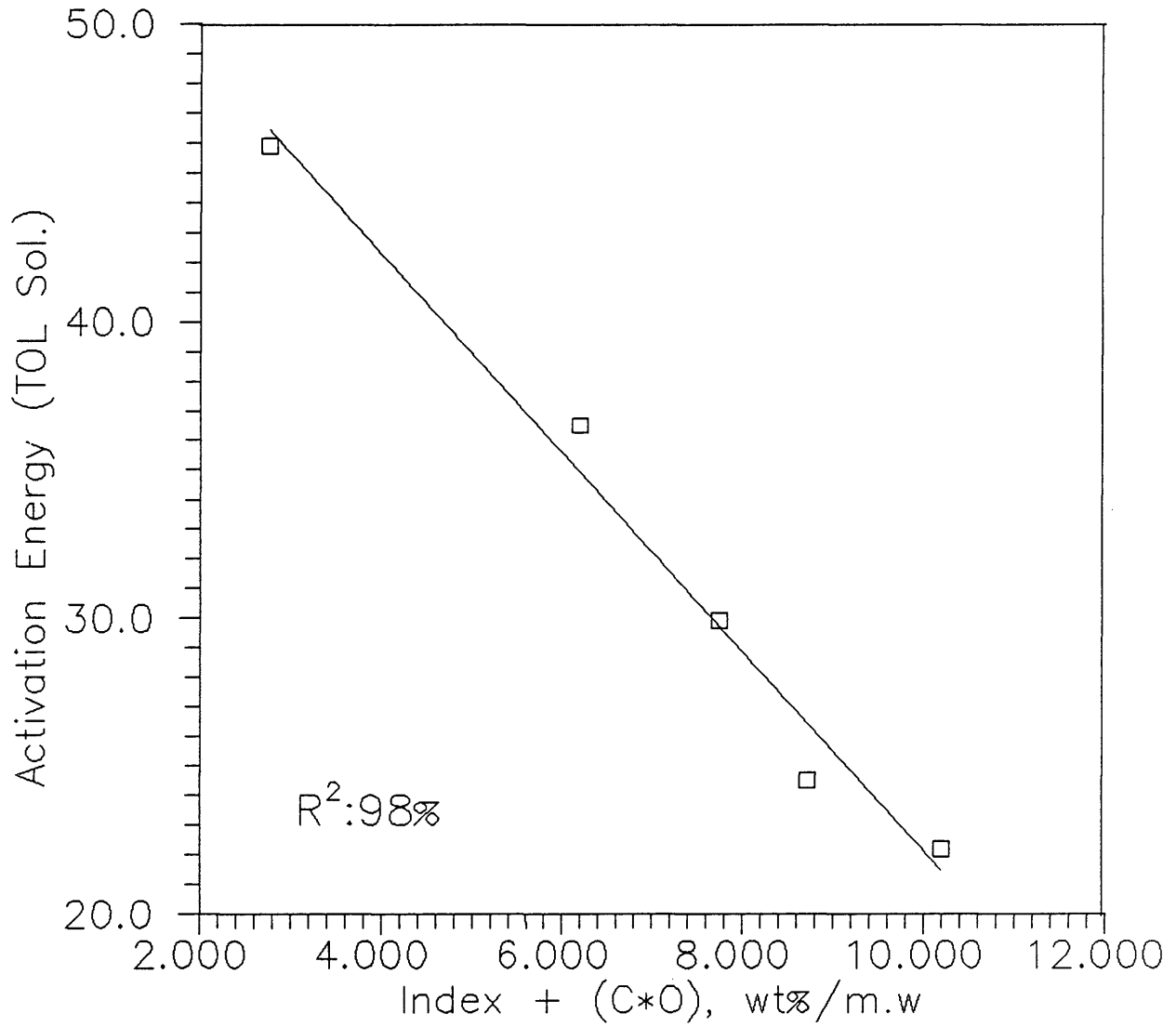


Figure 25. Correlation of Activation Energy vs. Index+(C*O)
(Toluene Solubles)

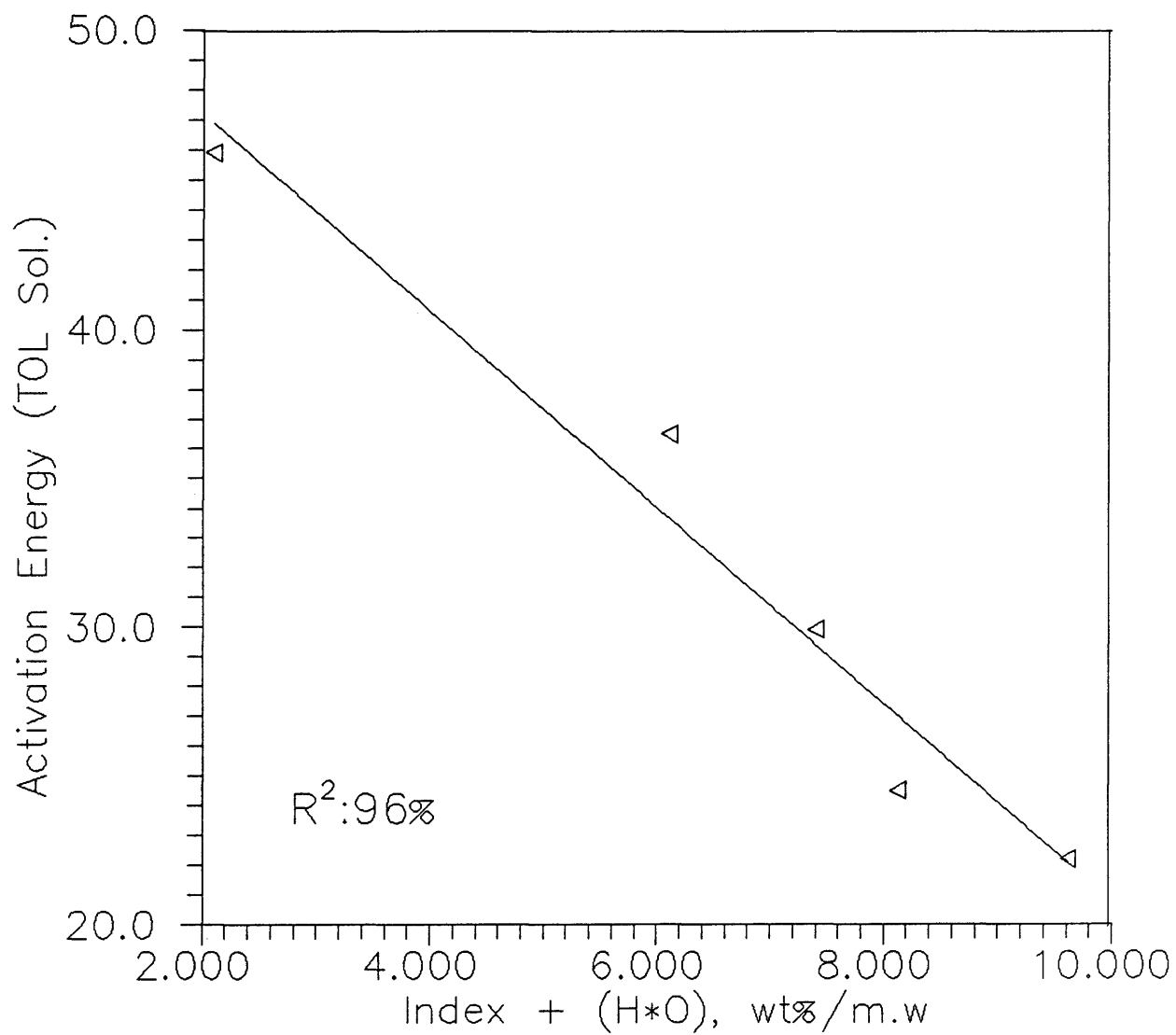


Figure 26. Correlation of Activation Energy vs. Index+(H*O)
(Toluene Solubles)

properties. This parameter was found to be highly correlated with the following variables:

$$\ln(k_0) (\text{THF}) = 39.2 - 2.20 (\text{Index} + \text{C}) \quad \text{R-sq:86\%}$$

$$\ln(k_0) (\text{TOL}) = 36.2 - 2.53 [\text{Index} + (\text{C} * \text{O})] \quad \text{R-sq:98\%}$$

where, k_0 = Frequency factor (1/min)

Index = Free swelling index

C,O = Total Carbon and Oxygen (wt%/m.w, d.a.f)

Since both frequency factor and activation energy are highly correlated with the same variables, a predictive equation for the rate constant may be developed by using the Arrhenius equation:

$$\ln k = \ln k_0 - E/RT$$

$$\ln k(\text{THF Sol}) = [39.2 - 2.20 (I + C)] - 1/RT [55.6 - 2.66 (I + C)]$$

$$\ln k(\text{TOL Sol}) = \{36.2 - 2.53 [I + (C * O)]\} - 1/RT \{55.7 - 3.36 [I + (C * O)]\}$$

where, k = Kinetic constant (1/min)

I = Free swelling index

C,O = Total Carbon and Oxygen (wt%/m.w, d.a.f)

By using these two predicting equations for rate constants to THF and toluene solubles, observed values and predicted values were correlated. The predicted rate constant for THF solubles was correlated well with the observed value (R-sq 90%), but correlation for toluene solubles was not as good

(R-sq 51%). These results are presented in Figures 27 and 28 in the form of parity plots. Correlations for activation energy and frequency factor with coal properties are shown in Table 13. The finding that activation energies for conversion to THF and toluene solubles depend strongly on the free swelling index, total carbon, and total oxygen contents could give some insight into the chemical structure of coal. The activation energy for a chemical reaction shows the level of energy required to initiate the reaction. It is known that the reaction of coal liquefaction is initiated by breaking the bridging bonds between macromolecular units first, since they are the weakest bonds in coal. Hence, activation energy should be higher for coals which are more strongly cross-linked. From the correlation of activation energy for conversion to THF solubles, we see that this parameter is correlated with free swelling index which is in turn directly related to the degree of cross-linking in coal. However activation energy was not uniquely correlated with free swelling index alone. Independent variables found to be significant include total carbon and hydrogen too. It thus could be suggested that the activation energy for coal conversion to THF solubles was correlated with the cross-linking of aliphatic carbon. For the toluene solubles, activation energy was a function of oxygen content in addition to free swelling index, carbon, and

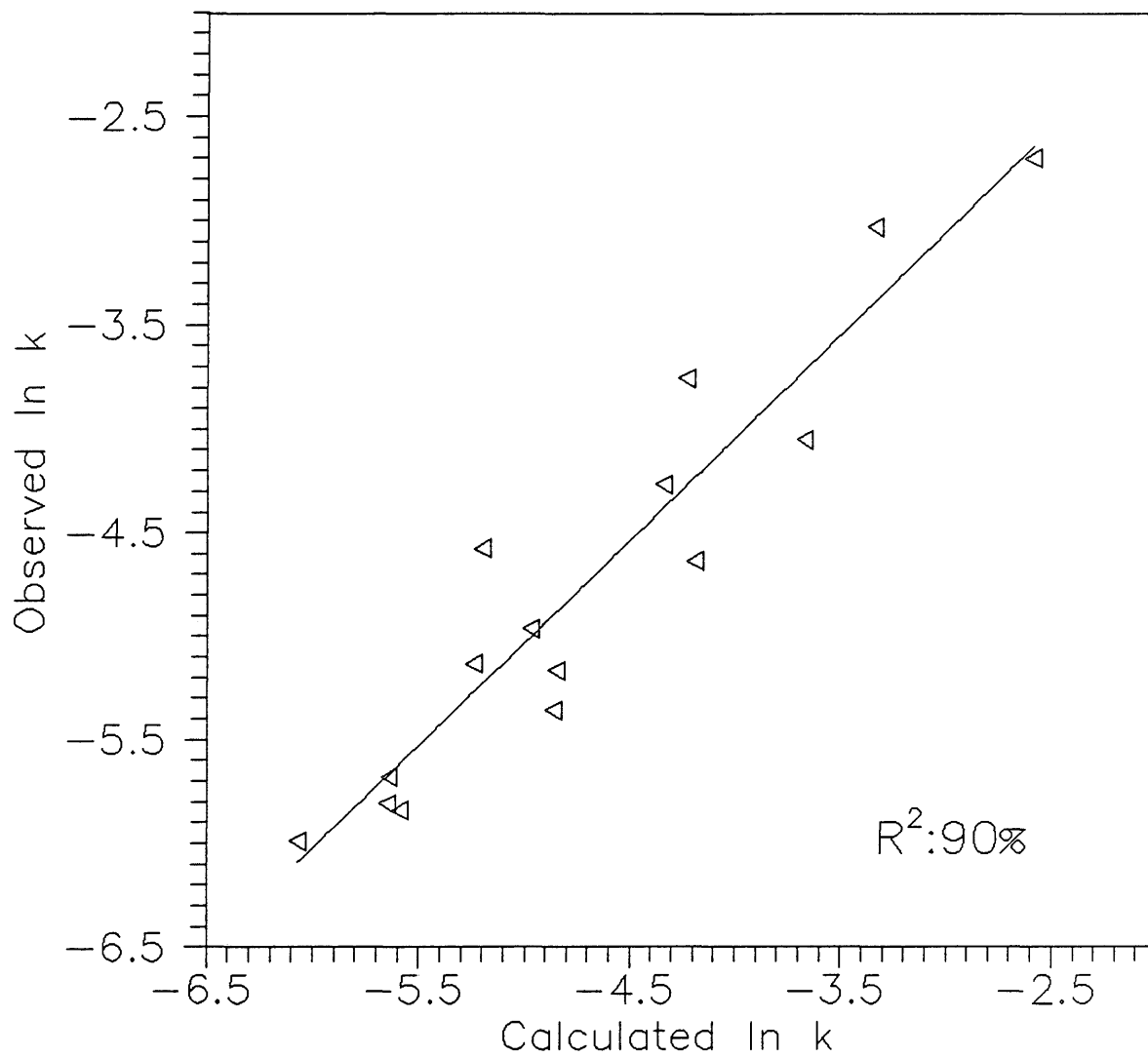


Figure 27. Correlation of Observed and Calculated Rate Constants (THF Solubles)

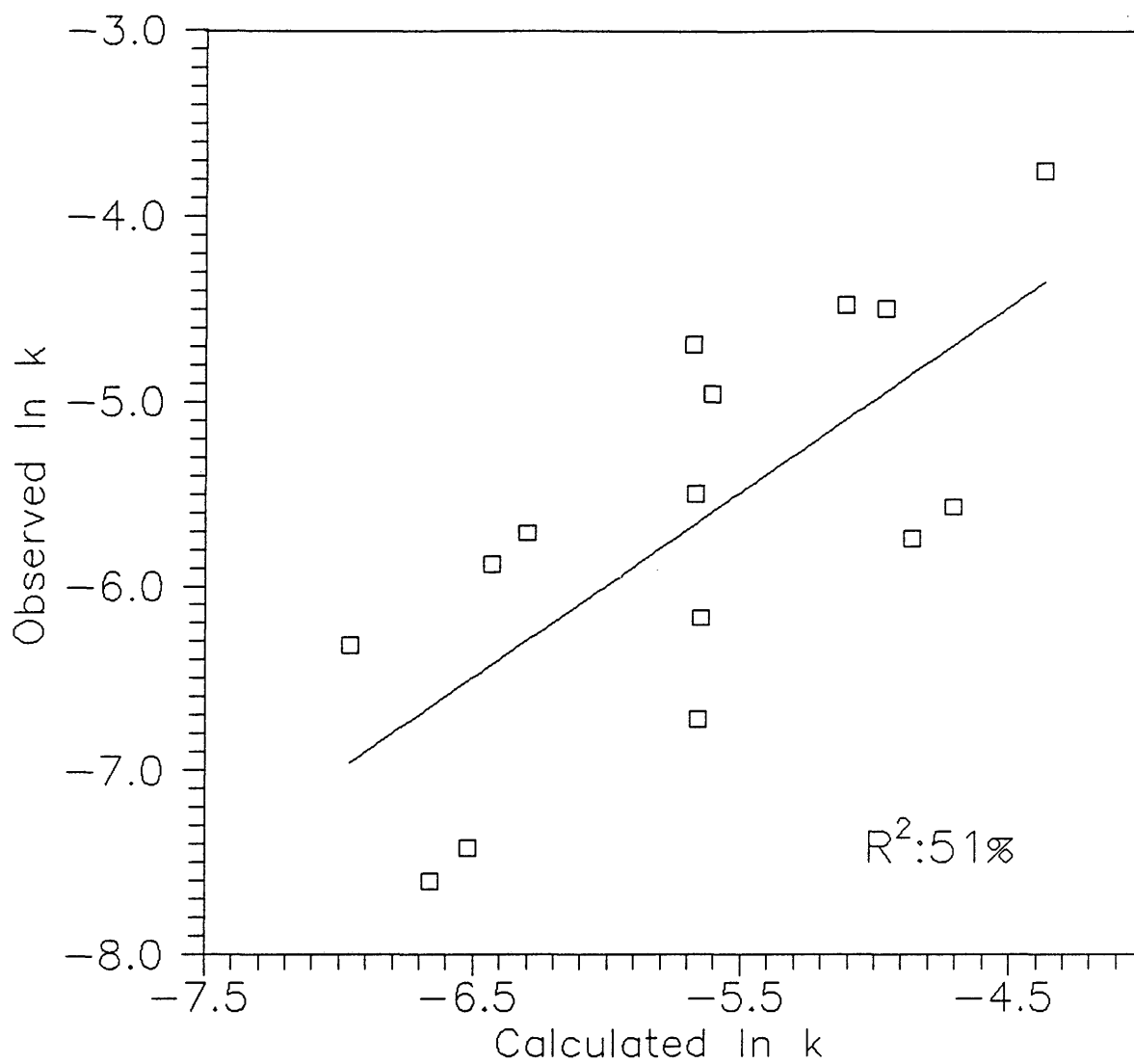


Figure 28. Correlation of Observed and Calculated Rate Constants (Toluene Solubles)

Table 13. Correlations of Activation Energy, Frequency
Factor with Coal Properties

Multiple Correlation Coefficients

Property*	E(Tol)	E(THF)	k0(Tol)	k0(THF)	lnk0(Tol)	lnk0(THF)
C	18	58	34	64	22	53
H	29	3	83	0	39	5
O	25	62	8	96	22	60
N	26	4	80	1	34	6
S	7	2	10	19	3	3
C+H	1	93	0	86	1	93
C*H	0	89	4	75	1	91
C*H	26	58	7	94	23	56
I+C	6	82	11	56	7	86
I+(C*H)	4	82	12	60	6	86
I+(H*O)	96	2	80	8	98	4
I+(C*O)	98	2	74	10	98	3

* Property values (wt%/m.w, d.a.f)

where, E = Activation energy (kcal/mole)

k0= Frequency factor (1/min)

I = Free Swelling Index

hydrogen. This implies that activation energy for conversion to toluene solubles is a function of aliphatic carbon and oxygen, hence suggesting the importance of aliphatic ether groups in cross-linking structures.

6. CONCLUSIONS

* Activation energy obtained using a second order reversible kinetic model was not linearly correlated with a single property of coal, but it is strongly correlated with combinations of fundamental properties e.g. (C+H) or [I+(C*O)].

* It was shown that the reactivity ranking of coals by activation energy was independent of the kinetic model used.

* Total carbon, hydrogen, and free swelling index were found to be important properties in predicting activation energy for conversion of coal to THF solubles.

* A universal correlation for rate constants including temperature effects was derived. The total carbon and free swelling index were very important properties in predicting the rate constant for conversion to THF solubles.

7. RECOMMENDATIONS

For more general results the method and correlations used in this study should be tested by applying to a greater number of coal samples.

Activation energy dependence should be tested with other coal functionalities e.g. aliphatic carbon, hydrogen content and aromatic carbon, hydrogen content.

LITERATURE CITED

1. Whitehurst, D.D, Mitchell, T.O, Farcasiu, M, "Coal Liquefaction. The Chemistry and technology of Thermal Processes", Academic Press, Ch.1, (1980)
2. Gorbaty, M.L, Ouchi, K, "Coal Structure", Advances in Chemistry Series, American Chemical Society, Washington, D.C. (1981)
3. Shah, Y.T, "Reaction Engineering in Direct Coal Liquefaction", Addison-Wesley Pub.Comp. Ch.2, P.39 (1981)
4. Schweighardt, F.K, Thames, B.M, "Solvent Extraction of Coal Derived Products", Anal.Chem., v.50, p.1381 (1978)
5. Miller, R.L, Wasden, F.K, "Comparison of Experimental Solvent Extraction Techniques to Determine the Apparent Composition of Solvent Refined Coal", Fuel Processing Technology, v.9, p.117 (1984)
6. Schwager, I, Yen, T.F, "Coal-liquefaction Products from Major Demonstration Process. 1. Separation and Analysis", Fuel, v.57, p.100 (1978)
7. Petrakis, L, Grandy, D.W, Jones, G.L, "Free Radicals in Coal and Coal Conversions. 7. An in-depth Experimental Investigation and Statistical Correlative Model of the Effects of Residence Time, Temperature and Solvents", Fuel, v.61, p.21 (1982)
8. Benjamin, B.M, et al, "Thermal Cleavage of Chemical Bonds in Selected Coal-related Structures", Fuel, v.57, p.269 (1978)
9. Poutsma, M.L, "Free-radical Model for Coal Conversions. Effect of Conversion Level and Concentration on Thermalysis of Bibenzyl", Fuel, v.59, p.335 (1980)
10. Korobkov, V.Y, et al, "Effect of the Structure of Coal-related Model Ethers on the Rate and Mechanism of Their Thermolysis. 1. Effect of the Number of Methylene Groups in the $R-(CH_2)_n-O-(CH_2)_m-R$ Structure Fuel, v.67, p.657 (1988)
11. Korobkov, V.Y, et al, "Effect of the Structure of Coal-related Model Ethers on the Rate and Mechanism of Their Thermolysis. 2. Effects of Substituents in the $Ph-CH_2-O-Ph-X$ Structure", Fuel, v.67, p.663 (1988)

12. Cassidy, P.J, Jackson, W.R, Lackins, F.P, "Hydrogenation of Brown Coal. IV.Model Compound Studies and Mechanistic Considerations", Fuel, v.62, p.1404 (1983)
13. Takemura, Y, Itoh, H, Ouchi, K, "Hydrogenalysis of Coal-related Model Compounds by Carbon Monoxide-Water Mixture ", Fuel, v.60, p.379 (1981)
14. Matsushashi, H, Hattari, H, and Tanebe, K, "Catalitic Activities of Binary Metal Oxides Containing Iron Hydrocracking of Benzyl Phenyl Ether and Diphenyl Ether", Fuel, v.64, p.1224 (1985)
15. Kamiya, Y.K, Nagae, S, Oikawa, "Effect of Coal Minerals on the Thermal Treatment of Aromatic Ethers and Carbonyl Compounds ", Fuel,v.62, p.30 (1983)
16. Yoshida, T, Tokuhashi, K, Maekaea, Y, "Liquefaction of Coal.1. Depolymerization of Coal by Cleavages of Ether and Methylene Bridges", Fuel, v.64, p.890 (1985)
17. Kamiya, Y et al, "Thermal Cracking of Coal Model Diaryl Ethers in Aromatic Solvent", Fuel, v.65, p.586 (1986)
18. Schlosberg, R.H, et al, "Pyrolysis of Benzyl Ether Under Hydrogen Starvation Conditions",Fuel, v.60, p.155 (1981)
19. Neill, P.H, et al, "Dependence of Coal Liquefaction Behavior on Coal Characteristics. 9.Ligeufaction of a Large Set of High-Sulphur Coal Samples", Fuel, v.67, p.1459 (1988)
20. Larsen, J.W, "Coal Structure", American Institue of Physics, Ch.1 (1981)
21. Larsen, J.W, Lee, D, "Steric Requirements for Coal Swelling by Amine Bases", Fuel v.64, p.981 (1985)
22. Ouchi, K, Ohe, S, Makabe, M, Itoh, H, "Reaction Mechanism of Coal Hydrogenation. 3.Effect of Coal Type", Fuel, v.67, p.1391 (1985)
23. Shin, S-C, "Corelation of Coal Hydroliquefaction Rate with Coal Properties", Ph.D. Thesis T-3569, Colorado School of Mines, Golden, C.O. (1988)

24. Neavel, R.C, "Liquefaction of Coal in Hydrogen-donor and non-donor Vehicles", Fuel v.55, p.237 (1976)
25. Utz, B.R, et al, "The Roles of Vehicle and Gaseous Hydrogen During Short Contact Time Coal Liquefaction", Fuel, v.65, p.1085 (1986)
26. Winschel, R.A, et al, "Corelation of Microautoclave H n.m.r Measurements of Coal Liquefaction Solvent Quality", Fuel, v.65, p.526 (1986)
27. Given, P.H, et al, "Chemical Properties of Coal Macerals I-Introductory Survey, and Some Properties of Exinites", Fuel, v.39, p.323 (1960)
28. Brown, J.K, J.Chem.Soc. p.752 (1955)
29. Abdel-Baset, Z, Given, P.H, Yarzab, R.F, "Re-examination of the Phenolic Hydroxyl Contents of Coals", Fuel, v.57, p.95 (1978)
30. Kamiya, Y, Sato, H, Yao, T, "Effect of Phenolic Compounds on Liquefaction of Coal in the Presence of Hydrogen-donor Solvent", Fuel, v.57, p.681 (1978)
31. Storch, H.H, et al, "Hydrogenation of a Pittsburgh Seam Coal", IEC, v.32, p.346 (1940)
32. Oelert, H-H, Sieckmann, R, "Liquefaction of Coal and Related Materials", Fuel, v.55, p.39 (1976)
33. Oele, A.P, et al, "Extractive Disintegration of Bituminous Coals", Fuel, v.30, p.169 (1951)
34. Hill, G.R, Anderson, L.L, Shifai, M.Y, "Activated Extraction of Coal Using a Hydrogen-donor Solvent", Fuel, v.53, p.32 (1974)
35. Cronauer, D.C, Shah, Y.T, Ruberto, R.G, "Kinetics of Thermal Liquefaction of Belle Ayr Subbituminous Coal", IEC Proc. Des. Dev., v.17, p.281 (1978)
36. Given, P.H, et al, "Dependence of Coal Liquefaction Behavior on Coal Characteristics. 1. Vitrinite-rich Samples", Fuel, v.54, p.34 (1975)
37. Given, P.H, et al, "Dependence of Coal Liquefaction Behavior on Coal Characteristics. 2. Role of Petrographic Composition", Fuel, v.54, p.40 (1975)

38. Abdel-Baset, M.B, Yarzab, R.F, Given, P.H, "Dependence of Coal Liquefaction Behavior on Coal Characteristics. 3. Statistical Corelation of Conversion in Coal-tetralin Interaction", Fuel, v.57, p.89 (1978)
39. Yarzab, R.F, Given, P.H, Spackman, W, Davis, A, "Dependence of Coal Liquefaction Behavior on Coal Characteristics. 4. Cluster Analysis for Characteristics of 104 Coals", Fuel, v.59, p.81 (1980)
40. Furlong, M.W, "Corelation of Parent Coal Properties With a Kinetically-Defined Donor Solvent Liquefaction Reactivity" Ph.D. Thesis T-2472, Colorado School of Mines, Golden, C.O. (April 1981)
41. Baldwin, R.M, Voorhees, K.J, Durfee, S.L, "Relationship of Coal Characteristics to Coal Reactivity for Direct Hydrogenation Liquefaction", Fuel Processing Technology, v.15, p.281 (1987)
42. Shalabi, M.A, Baldwin, R.M, Bain, R.L, Gary, J.H, Golden, J.O, "Noncatalytic Coal Liquefaction in a Donor Solvent. Rate of Formation of Oil,Asphaltenes, and Preasphaltenes",IEC Proc. Des.Dev., v.18, p.474 (1978)
43. Nishida, N, "Qualitative & Quantitative Assessment of Reaction Models of Coal Hydrogenation", Fuel Processing Technology, v.3, p.231 (1980)
44. Szladow, A.J, Given, P.H, "Models and Activation Energies for Coal Liquefaction Reactions", IEC Proc. Des. Dev., v.20, p.27 (1981)
45. Anthony, D.B, et al, "Rapid Devolatilization of Pulverized Coal", Fifteenth Symposium (International) on Combustion, p.1303 , The Combustion Institute, Pittsburgh, PA. (1975)
46. Anthony, D.B, Howard, J.B, "Coal Devolatilization and Hydrogasification ", AIChE J., v.22, p.625 (1976)
47. Neavel, R.C, et al, "Interrelationships Between Coal Compositional Parameters", Fuel, v.65, p.312 (1986)
48. Neill, P.H, Shadle, L.J, Given, P.H, "Dependence of Coal Liquefaction Behaviour on Coal Characteristics. 9. Liquefaction of a Large Set of High-Sulphur Coal Samples", Fuel, v.67, p.1459 (1988)

49. Shalde, L.J, Neill, P.H, Given P.H, "Dependence of Liquefaction Behaviour on Coal Characteristics.10. Structural Characteristics of a Set of High-Sulphur Coals and the Asphaltenes Derived from Them", Fuel, v.67, p.1465 (1988)
50. Curran, G.P, Struck, R.T, Gorin, E, "Mchanism of the Hydrogen Transfer Process to Coal and Coal Extract", I&EC Pro. Des. Dev., v.6, p.166 (1967)
51. Wisler, W.H, "A Kinetic Comparison of Coal Pyrolysis and Coal Dissolution", Fuel, v.47, p.475 (1968)
52. Shah, V.T, Cronauer, D.C, McIlvried, H.G, Paraskos, J.A, "Kinetics of Catalytic Liquefaction of Big Horn Coal in a Segmanted Bed Reactor", IEC Proc. Des. Dev., v.17, p.288 (1978)
53. Shin, S-C, Baldwin, R.M, and Miller, R.L, "Coal Reactivity in Direct Hydrogenation Liquefaction Process: Measurament and Correlation with Coal Properties", Fuel, v.1, p.377 (1987)
54. Fischer, C.H, Sprunk, G.C, Eisner, A, Clarke, L, Fein, M.L, Storch, H.H, "Hydrogenation of Anthraxylon (Vitrain) from Peat, Brown Coal, Lignite, Sub-bituminous Coal and Anthracite. The Effect of Rank in Coal Hydrogenation", Fuel, v.19, p.132 (1940)
55. Cooper, B.R, Ellingson, W.A, "The Science and Technology of coal and Coal Utilization", Plenum Press, New York and London, (1984)
56. Fischer, C.H, Sprunk, G.C, Eisner, A, O'Donnell, H.J, Clarke, L, Storch, H.H, "Hydrogenation and Liquefaction of Coal. Part 2. Effect of Petrographic Composition and Rank of Coal", U.S. Bureau of Mines Technical Paper 642 (1942)
57. Kessler, M.F, "Interpretation of the Chemical Composition of Bituminous Coal Macerals", Fuel, v.52, p.191 (1973)
58. Furlong, M.W, Baldwin, R.M, and Bain, R.L, "Reactivity of Coal Towards Hydrogenation-Ranking by Kinetic Measurements", Fuel, v.61, p.116 (1982)
59. Neill, P.H, et al, "A Search for Systematic Relations Between Aromaticity and Ranf of High Sulfur Coals", Fuel, v.66, p.92 (1987)

60. Neill, P.H, et al, "Aromaticity of Some High Sulfur Coals: Surprising Degree of Heterogeneity", Fuel, v.66, p.96 (1987)
61. Neavel, R.C, "Coal Science: an Idiosyncratic View", Fuel, v.65, p.1632 (1986)
62. Prasad, G.N, et al, "Modeling of Coal Liquefaction Kinetics Based on Reactions in Continious Mixtures. Part 2. Comparision with Experiments on Catalyzed and Uncatalyzed Liquefaction of Coals of Differant Rank", AIChE J, v.32, p.1288 (1986)
63. Gutmann, M, et al, "Correlation Between Parameters of Lignite and Hydrogenation Reactivity from Experiments in a Batch Reactor", 1987 International Conferance on Coal Science, p.187
64. Vernon, L.W, "Free Radical Chemistry of Coal Liquefaction: Role of Molecular Hydrogen", Fuel, v.59 p.102 (1980)
65. Guin, J.A, et al. "Further Studies of Catalytic Activity of Coal Minerals in Coal Liquefaction. 2. Performance of Iron and SRC Mineral Residue, as Catalysts and Sulfur Scavengers", Ind. Eng. Chem. Process Des. Dev, vol.18, No.4, p.631 (1979)
66. Baldwin, R.M, and Vinciguerra, S, "Coal Liquefaction Catalysis. Iron Pyrite and Hydrogen Sulfide", Fuel, v.62, p.498 (1983)
67. Rolmann, L.D, ACS Preprints, Division of Fuel Chemistry, 21, p.59 (1976)
68. Mukherjee, D.K, and Chowdury, P.B, Fuel, vol.55, p.4 (1976)
69. Gates, Bruce C, "Liquefied Coal by Hydrogenation", Chemtech, p.99, February (1979)

APPENDIX

1. Kinetic data for five Penn State Coal Bank samples
2. Solutions of kinetic models
 - o First-second order reversible model
 - o Second order reversible model.
3. Computer program for the calculation of SEE.

Appendix 1-1. Kinetic Data for Weir-Pittsburg Coal

Conversion: d.a.f. basis wt %

TEMP(C)	CONVERSIONS	REACTION TIME, MIN				
		3 min	5 min	10 min	15 min	40 min
425	THF Conve	65	82	87	85	85
	TOL Conve	28	41	53	58	70
400	THF Conve	50	69	83	85	88
	TOL Conve	19	28	44	50	66
375	THF Conve	30	48	69	78	84
	TOL Conve	5	11	18	24	33

Appendix 1-2. Kinetic Data for Bevier-Wheeler Coal

Conversion: d.a.f. basis, wt%

TEMP(C)	CONVERSION	REACTION TIME,MIN				
		3 min	5 min	10 min	15 min	40 min
425	THF Conv	59	73	79	81	79
	TOL Conv	18	27	40	44	58
400	THF Conv	41	61	75	77	86
	TOL Conv	4	15	22	29	52
375	THF Conv	32	50	63	73	83
	TOL Conv	4	12	16	16	28

Appendix 1-3. Kinetic Data for Lower Sudduth Coal

Conversion: d.a.f. basis, wt%

TEMP (C)	CONVERSION	REACTION TIME, MIN				
		3 min	5 min	10 min	15 min	40 min
425	THF Conv	38	38	39	39	41
	TOL Conv	21	27	33	33	38
400	THF Conv	28	33	38	39	41
	TOL Conv	14	16	24	27	33
375	THF Conv	17	24	30	31	39
	TOL Conv	10	14	19	19	24

Appendix 1-4. Kinetic Data for Splashdam Coal

Conversion: d.a.f. basis, wt%

```
=====
```

TEMP(C)	CONVERSION	REACTION TIME,MIN				
		3 min	5 min	10 min	15 min	40 min
425	THF Conv	43	47	56	57	70
	TOL Conv	17	18	19	23	28

400	THF Conv	34	39	49	49	68
	TOL Conv	16	17	18	20	27

375	THF Conv	27	27	34	39	39
	TOL Conv	7	10	11	11	16

```
=====
```

Appendix 1-5. Kinetic Data for Lower Freeport Coal

Conversion: d.a.f. basis, wt%

```
=====
```

TEMP(C)	CONVERSION	REACTION TIME, MIN				
		3 min	5 min	10 min	15 min	40 min
425	THF Conv	25	28	30	30	25
	TOL Conv	10	11	11	16	15

400	THF Conv	22	26	28	28	31
	TOL Conv	3	7	10	10	12

375	THF Conv	16	20	21	25	25
	TOL Conv	2	2	5	6	6

```
=====
```


Appendix 2. Solutions of Kinetic Models

o First-Second Order Reversible Model

$$X = \frac{a \cdot X_e \cdot [1 - \exp(-Q \cdot t)]}{a + (a - X_e) \cdot \exp(-Q \cdot t)}$$

where, a : Ultimate conversion

X : Equilibrium conversion

t : Time

k_f : Forward kinetic constant

$$Q = k_f \cdot (2a - X_e) / X_e$$

o Second Order Reversible Model

$$X = \frac{a}{(1 - Q^2)} \cdot \left\{ 1 + Q \cdot \left[\frac{1 - P \cdot \exp(R \cdot t)}{1 + P \cdot \exp(R \cdot t)} \right] \right\}$$

where , $P = a / (a - 2X_e)$

$$Q = (a - X_e) / X_e$$

$$R = 2k \cdot a \cdot Q$$

Appendix 3. Computer Program for the Calculation of SEE

```

PROGRAM SEC-REVERSIBLE
DEMENSION XSTA(1000),DIF(1000),T(5),X(5),Q(1000),R(1000)
+           ,P(1000)
C           XSTA=CONVERSION FROM MODEL
C           DIF=DIFFERENCE BETWEEN CONVERSIONS FROM MODEL
C           AND EXPERIMENT
C           T(I)=TIME
C           X(I)=EXPERIMENTAL CONVERSION
REAL KIN,KF,N,K,I
C *****

WRITE(*,*) 'ASSUME INITIAL,B,AND FINAL,F,ULTIMATE CONV'
READ(*,*) B,F
C *****

WRITE(*,*) 'ASSUME INITIAL,XIN,AND FINAL,XF,EQUILI CONV'
READ(*,*) XIN,XF
C *****

WRITE(*,*) 'ASSUME INITIAL,KIN,AND FINAL,KF,KINETIC CONS'
READ(*,*) KIN,KF
C *****

OPEN(UNIT=2,FILE='TIME425TH1.DAT',STATUS='OLD')
OPEN(UNIT=3,FILE='SREVV425TH1.OUT',STATUS='NEW')
N=5.0

DO I=1,5
READ(2,*) T(I),X(I)
ENDDO

DO A=B,F
DO E=XIN,XF
DO K=KIN,KF,0.001

SUM1=0.0
DO I=1,5
Q(I)=(A-E)/E
R(I)=2*K*A*Q
P(I)=A/(A-2*E)

XSTA(I)=A/(1-Q(I)**2)*(1+Q(I)*((1-P(I)*EXP(R(I)*T(I)))/
+ (1+P(I)*EXP(R(I)*T(I))))))
DIF(I)=(X(I)-XSTA(I))**2
SUM1=SUM1+DIF(I)
ENDDO
STOPL=SQRT(SUM1)
SOLN=STOPL/N

```

```
WRITE(3,60) SOLN,A,E,K
60 FORMAT(1X,F8.4,1X,F5.2,1X,F8.4,1X,F8.4)
ENDDO
ENDDO
ENDDO
STOP
END
```